

Stable Simultaneous Stator and Rotor Resistances Identification for Speed Sensorless Induction Motor Drives: Review and New Results

Jiahao Chen, *Student Member, IEEE*, Jin Huang

Abstract—After a technical review on the stator resistance and rotor resistance identification methods for speed sensorless induction motor drives, this paper presents a different solution with a new representation of induction motor dynamics. In virtue of this representation, an adaptive observer is designed. The key step is to introduce the corrective terms and the filtered regressors, which forces the error dynamics of the observer to approach the ones in a form to which the Kalman-Yakubovich lemma can be applied. Only stator currents are required in the parameter adaptation rules. Particularly, the biased sinusoidal flux modulus command assures the convergence of parameters, and the consequent speed ripple problem is discussed. However, the above design has an imperfection and is found to be insufficient to assure stable operation in low-speed regeneration. Thus, further stability analysis based on the steady-state linearized model and remedies for stabilization are given. Effective experiment and simulation results are included.

Index Terms—adaptive observers, induction motors drives, sensorless control, parameter estimation, rotor time constant, regeneration, slow reversal test.

NOMENCLATURE

$\hat{\cdot}$, $\tilde{\cdot}$	For derived symbols, a hat $\hat{\cdot}$ and a tilde $\tilde{\cdot}$ stand for estimation and error quantities, respectively, e.g., $\tilde{\omega} = \omega - \hat{\omega}$.
$*$	An asterisk $*$ indicates the commanded quantities.
$M-T$	The $M-T$ frame designates the rotor field oriented frame, where M -axis is aligned with the rotor flux vector while the T -axis is 90° leading to the M -axis.
I, J	$I = I_2 = \begin{bmatrix} 1 & 0 \\ 0 & 1 \end{bmatrix}, J = \begin{bmatrix} 0 & -1 \\ 1 & 0 \end{bmatrix}$.

I. INTRODUCTION

THE adaptive output regulation problem of a speed sensorless induction motor (IM) is challenging, because the outputs (e.g., flux modulus and rotor speed) are not measured. In the traditional adaptive control problem with outputs available, the convergence of parameter adaptation is not necessary as long as the outputs are regulated to the commanded values. In speed sensorless IM drives, however, any uncertainty in stator resistance [1] or rotor resistance [2] detrimentally affects the control accuracy of the speed.

This work was supported in part by the National Key Basic Research Program of China (973 Project) under Grant 2013CB035604 and in part by the National Natural Science Foundation of China under Grant 51690182.

J. Chen and J. Huang are with the College of Electrical Engineering, Zhejiang University, Hangzhou 310027, China (e-mail: horychen@qq.com; ee_huangj@emb.zju.edu.cn).

The aim of the paper splits in two. The first is to provide a review of the development of the techniques used for both stator and rotor resistances identification in speed sensorless IM drives, while the other is to present a new solution. Please refer to Table I for a list of symbol definitions.

A. Technology Status Review on Resistances Identification in Speed Sensorless IM Drives

In a sensorless IM drive, there are two degrees of freedom available for parameter identification when IM is under constant flux modulus and constant speed operation [3], [4]. To be specific, one degree of freedom is occupied by r_s identification, while the other is taken by the identification of the lumped parameter $\omega + r_{req} \frac{T_L}{n_{pp} |\psi_\mu|^2}$, i.e., the synchronous angular speed. That is, the IM model is parameterized in a way that the rotor speed and the rotor resistance are not distinguishable. Therefore, at first, method i and ii seek for extra degree of freedom for parameter identification.

i) *Proportional Correction*. A proportional correction for \hat{r}_r with respect to the model-based estimation of r_s is suggested [5], so that the variation caused by temperature change is compensated. However, the correction can hardly be exact, and the variation in r_r owing to skin effect is not covered.

ii) *Speed Information Extraction from Magnetic Asymmetry*. Besides model-based speed estimation, speed can also be estimated from rotor slot harmonics [6]. However, the extraction of the rotor slot harmonics encounters vital problems during very low or very high speed operation, and furthermore, it only applies to some types of IMs. In addition, if high frequency signal injection is allowed, the speed can be recovered from the induced magnetic saliency, by rotating signal [7], or by fluctuating signal [8].

As a matter of fact, Marino et al. [9], [10] have pointed out that r_r can be distinguished from ω only when either the flux modulus or the rotor acceleration varies, which corresponds to method iii and method iv, respectively.

iii) *r_r Identification during Speed Transient*. Since flux modulus is not exactly constant during speed transient (e.g., when stator voltage equations are not exactly decoupled in the $M-T$ frame), both r_r and ω can be identified during speed transient [11], [12].

iv) *r_r Identified from the Mechanical Equation*. By noticing that r_r appears in the dynamic equation of the rotor acceleration, it can be identified if the torque producing current i_{Ts} is persistently exciting [13]. (Actually, a time-varying i_{Ts} suffices.)

TABLE I. List of Symbols

T-circuit Symbols	Notation	Comment
Stator resistance	r_s	3.04Ω
Rotor resistance	r_r	1.69Ω
Stator inductance	L_s	0.4826 H
Rotor inductance	L_r	0.4826 H
Magnetizing inductance	L_m	0.47 H
Stator voltage in $\alpha\beta$ frame	u_s	$u_s = [u_{\alpha s}, u_{\beta s}]^T$
Stator current in $\alpha\beta$ frame	i_s	$i_s = [i_{\alpha s}, i_{\beta s}]^T$
Rotor flux (linkage) in $\alpha\beta$ frame	ψ_r	$\psi_r = [\psi_{\alpha r}, \psi_{\beta r}]^T$
Inverse- Γ -circuit Symbols	Notation	Comment
Equivalent rotor resistance	r_{req}	$r_{req} = r_r L_m^2 / L_r^2$
Equivalent magnetizing inductance	L_μ	$L_\mu = L_m^2 / L_r$
Total leakage inductance	L_σ	$L_\sigma = L_s - L_\mu$
Equivalent rotor flux (linkage)	ψ_μ	$\psi_\mu = \psi_r L_m / L_r$
Other Symbols	Notation	Comment
Differentiation operator	p	$p = \frac{d}{dt}$
Number of pole pairs	n_{pp}	$n_{pp} = 2$
Load torque	T_L	-
Reciprocal of the rotor time constant	α	$\alpha = r_{req} / L_\mu$
Electrical angular rotor speed	ω	-
Synchronous angular speed	ω_ψ	-
Slip angular speed	ω_{sl}	$\omega_{sl} = \omega_\psi - \omega$

In order to cover the case when variation of r_r occurs at steady-state operation, method v, vi and vii add time-varying excitation onto the magnetizing current i_{Ms} [14], [15], [16], [17], [18]. To make the classification clear, method v, vi and vii may be termed as *index* or *evaluation function* based methods. That is, parameter information is extracted from the *index* that is derived with some assumptions or approximations. So, the results are valid under restricted conditions.

v) *Simplified Adaptation Rules (Full-order Observer)*. With a sinusoid superimposed onto the magnetizing current i_{Ms} , r_r is identified along with ω and r_s from the simplified adaptation rules derived from Lyapunov's theorem¹, i.e., the unknown flux estimated error is neglected in the adaptation rules [14], [15]. In their implementation, speed ripple exists owing to the time-varying magnetizing current.

vi) *Back-stepping based Observer*. A back-stepping based observer that is adaptive to r_s , r_{req} , L_μ and ω , has been proposed by Rasmussen et al. [16]², where a square wave is superimposed onto the magnetizing current i_{Ms} . However, the observer stability holds locally provided that initial errors of estimations are sufficiently small (so that the flux estimated error plus the current estimated error gives approximately a null vector, i.e., they have an opposite sign). Similarly, speed ripple exists.

vii) *Small Signal based Linear Approximations*. With a sinusoid superimposed onto the flux modulus command, r_r is computed from the linearly perturbed dynamics around a steady-state operating point [17]. Though the reconstruction of high order derivatives of signals is required, the scheme is complete, for it includes feedback linearizing control to eliminate speed ripples, and the identifiability of r_s and r_r is well interpreted and is retained regardless of load conditions.

¹The hyper-stability based counterpart is presented by Yang and Chin [19], where the ratio between the flux estimated error norm and the estimated current error norm is assumed to be bounded.

²A journal version of this back-stepping design by different authors can be found in [20].

See also [18] for a recent development of r_r identification based on the small signal approach.

Generally, for those *index* based methods, neither stability analysis nor parameter convergence for the overall system is justified, which is also the case for methods based on artificial neural network (ANN) or extended Kalman filter (EKF). Moreover, ANN and EKF consume more computation resources.

viii) *ANN based Approach*. With ω identified by some regular techniques, r_s and r_r can be separately [21] or conjointly [22] identified by ANN.

ix) *EKF with Variable Structure*. In stochastic setting, EKF is the choice for online identification of r_s , r_r and ω , and it is usually implemented in variable structure. For instance, there are switching EKF [23], braided EKF [24] and bi-input EKF [25], [26], among which bi-input EKF is believed to be of the most computational efficiency. Though the equivalence between adaptive observer (AO) and EKF has been revealed by Besançon et al. [27], [28], still, we will only concern AO rather than EKF, because of the limitations of EKF³.

Instability may result if a rigorous stability analysis is absent. For instance, adaptive full-order observer (method v) requires full states feedback in theory, and lack of flux measurement (utilizing only current estimated error) incurs instability during low speed regeneration [31]. This is a well-known problem and draws lots of attention in literatures. The stabilization can be achieved through the redesign of observer feedback gain and/or speed adaptation law. Techniques for analyzing the stability of the speed adaptive full-order observer, which takes feedback gain and adaptation law into account, may be categorized as follows.

- (1) *Lyapunov inequality based analysis* [32]. By means of a careful arrangement on the linear feedforward block and nonlinear feedback block [33] (cf. [19]), the conditions for hyper-stability are reduced to the positive real or the almost positive real property of the transfer function from speed estimated error to the output error. Particularly in [32], closed-form solutions of zeros and poles in terms of explicit design coefficients are derived, which are deemed to be very useful for further zero and pole allocation [e.g., to obtain sufficient damping at high speed (see also [34])].
- (2) *Complete stability conditions* [35]. With the assumption of fast convergence of speed estimation and current estimation, the full-order observer has its equivalent reduced-order implementation and inherently sensorless implementation as well as its *complete stability* conditions that are derived from the Routh-Hurwitz criterion and the (reduced-order) linearized error dynamics.
- (3) Analysis of the linearized model around steady-state operating point via root-locus plot or Routh-Hurwitz criterion. Specifically, linearization has been performed for the AO subsystem [36], both the AO subsystem and the controller subsystem [37], and the AO error dynamics [38], [39]. In [39], a standard stabilization procedure along with pertinent practical considerations is presented.

³As claimed in [29]: "Unfortunately, as an approximation, the EKF has various limitations, such as problems with covariance estimation and convergence for multi-dimensional, nonlinear models." (See also [30].)

However, as is illustrated in [39], stabilization through only feedback gain selection can be very parameter dependent. So, to enhance the robustness to parameter variation, it is suggested to also redesign speed adaptation law (see e.g., [40]), or to incorporate parameter adaptation—which is the topic of this paper. In contrast to those *index* based methods, method x begins to pay more attention to the stability issues, and method xi further concerns the condition of parameter convergence, i.e., the persistent excitation condition (PE condition).

x) *Adaptive Full-order Observer.* Recently, the Routh-Hurwitz criterion and root-locus based stability analysis of the estimation of ω and r_s [41] is extended for further inclusion of r_r identification [42], where the coupling among the estimation loops of ω , r_s and r_r is neglected for simplification. However, a different opinion is that, as stated in [41], [43], the coupling between ω and r_s estimation loops is the main cause of instability. To this end, the coupling among estimation loops of ω , r_s and r_r is considered in [44]⁴.

xi) *Adaptive Flux Observer.* A time division multiplexing (TDM) based flux observer is presented in [45], where a DC biased trapezoidal flux modulus command is imposed, so that the 3rd order PE condition of ω , r_s and r_r is reduced to two 2nd order ones. By treating one resistance error (to which the adaptation is suspended) as the disturbance, rigorous input-to-state stability and convergence analysis are conducted. The so-called TDM approach *per se* is based on the variable structure concept similar to those methods of variable structure EKF, but the former features in the design of the decoupled identifiability of r_s with respect to uncertainty in r_r and ω .

For those speed adaptive observers introduced so far, a recapitulation follows:

- The rotor speed is treated as a model parameter, and to derive the speed adaptation law, the constant rotor speed assumption is necessary.
- Stabilization of speed estimation can be achieved in the local.
- It is implied that, unfortunately, the global asymptotic stability in the sense of Lyapunov is not attained, as shown in [46].

An interesting perspective is that, for Lyapunov stability based AO design, the unavailable flux estimated error is required only because the unknown parameters r_s , r_r and ω appear in the dynamics of the fluxes. Bear this in mind, it comes to method xii, where the rotor speed is treated as a state rather than a parameter and hence is not restricted to be time-invariant.

xii) *Nonlinear Observer of Current & Speed with Auxiliary States.* Assuming r_s is known, a nonlinear observer that estimates ω , r_r and T_L is designed in [10], where by introducing the auxiliary states $z = i_s + L_\sigma^{-1}\psi_\mu$, only current estimated error is theoretically needed to drive the estimation of r_r and ω , because the dynamics of z do not depend on r_r and ω .

⁴It is worth noting that the dynamics of estimated errors of parameters, which are first adopted in [43], are mainly concerned in the studies of [41], [44], while the transfer functions from estimated errors of parameters to the output errors [33] are analyzed in [42], rather than the linearized model.

Furthermore, if the auxiliary states are chosen as [47], [48]

$$z = i_s + L_\sigma^{-1} \left(\psi_\mu + r_s \int_0^t i_s dt \right)$$

then r_s disappears from the dynamics of z , too. However, integration of current is needed and the consequent IM model is over-parameterized by $r_s r_r$ and $r_s \omega$ [49], [50]. So, it has made this choice less popular. As a result, in [51], [52], based on the preliminary work of [10], the time-scale separation of r_s identification is further added to compensate r_s variation, where, presuming r_s known⁵, the PE condition is satisfied by a time-varying flux modulus and a rotating field. However, the identifiability of r_s holds locally and can not be checked *a priori* [52].

Remark: The adaptation rules of [10], [51], [52] are much more involved, because the composite observer-controller stability analysis is performed rather than the solo observer stability analysis, while the latter is the case for all other methods.

B. Proposed Adaptive Observer with the New State Variables

In stable adaptive system theory, the adaptive observer design with only outputs available involves a class of systems that can be transformed into the *adaptive observer form* [55], where the single-input single-output (SISO) system with the following error dynamics is considered

$$\begin{aligned} p\tilde{x} &= (A_c - KC_c)\tilde{x} + b\beta(y, u)^T\tilde{\theta} \\ y &= C_c x, \quad y, u \in \mathbb{R} \end{aligned} \quad (1)$$

where $x, \tilde{x} \in \mathbb{R}^n$, $\tilde{\theta} \in \mathbb{R}^p$, $\beta : \mathbb{R} \times \mathbb{R} \rightarrow \mathbb{R}^p$, $b \in \mathbb{R}^n$ is a constant vector, y the output, u the input, $C_c = [1 \ 0 \ \dots \ 0]$, $K \in \mathbb{R}^n$ is the pole allocation vector, and A_c is soon defined. The error dynamics (1) have the following properties:

- (i) The transformed system is in the form of Brunovsky, i.e., matrix A_c in the homogeneous part is
$$A_c = \begin{bmatrix} 0 & I_{n-1} \\ 0 & 0 \end{bmatrix}.$$
- (ii) The regressor $b\beta(y, u)$ consists of only known signals, or equivalently, the error dynamics are in the observable canonical form, i.e., $A_c - KC_c = \begin{bmatrix} -K & I_{n-1} \\ 0 & 0 \end{bmatrix}$.
- (iii) The error vector of parameters (denoted by $\tilde{\theta}$) enters each equation of system output and unmeasured states in the same manner, i.e., the term $\beta(y, u)^T\tilde{\theta}$ is a scalar. (It may differ up to a constant multiplier specified by b .)

However, neither the IM dynamics with fluxes ψ_μ as states nor those with auxiliary states z have these properties. This fact motivates the proposed adaptive observer design.

In this paper, we devise an adaptive observer with total leakage flux ψ_σ and electromotive force e as states. The new state equations meet property (i)⁶, but violate property (ii)

⁵In [53], [54], with the measurements of rotor speed and currents, adaptive designs with respect to r_s , r_r and T_L are presented, where in order to correspond PE conditions to motor operating conditions, r_s is also assumed to be known.

⁶The properties are extended to the case of the multiple-input multiple-output systems.

since the regressive part contains e , the unmeasured states. Fortunately, the counter-measure to this violation is carried out. Then, by a proper design of corrective terms and filtered regressors, the main design heuristics are to force the error dynamics of the devised observer approach the ones in a form to which the multi-variable Kalman-Yakubovich lemma can be applied [i.e., it fulfills property (iii)]. Particularly, the biased sinusoidal flux modulus command is needed for assuring the convergence of parameters. The speed ripples caused by the time-varying flux modulus can be alleviated from the control perspectives.

Paper structure follows. The observer design is covered in Sec. II. The whole system is introduced in Sec. III. The stability improvement in regeneration mode is delineated in Sec. IV. Finally, the discussion and the conclusion are placed in Sec. V and Sec. VI, respectively.

II. ADAPTIVE OBSERVER DESIGN

A. Mathematic Models

Neglecting mechanical friction, the symmetric and non-saturated IM dynamics in the stationary $\alpha\text{-}\beta$ frame are (2)

$$L_\sigma p i_s = u_s - r_s i_s - p \psi_\mu \quad (2a)$$

$$p \psi_\mu = r_{req} (i_s - L_\mu^{-1} \psi_\mu) + \omega J \psi_\mu \quad (2b)$$

$$J_s n_{pp}^{-1} p \omega = n_{pp} (i_s^T J \psi_\mu) - T_L \quad (2c)$$

where $p = \frac{d}{dt}$ is the differential operator, J_s is the moment of inertia, and inverse- Γ circuit parametrization is adopted [56] (see Table I). Note that (2c) implies the using of power invariant Clarke transformation.

B. Observer with Total Leakage Flux and Electromotive Force as States

Define the new state variables as $\psi_\sigma \triangleq L_\sigma i_s$ and $e \triangleq -p \psi_\mu$, and the electrical part of the IM dynamics is described by

$$\begin{aligned} p \psi_\sigma &= u_s - r_s i_s + e \\ p e &= -r_{req} (p i_s + L_\mu^{-1} e) + \omega J e \end{aligned} \quad (3)$$

where we have made assumptions of the constant electrical parameters and the natural time-scale separation between electrical dynamics and mechanical dynamics such that $p \omega = 0$ [57]. Please note that (3) is in the form of Brunovsky if we view it as follows

$$\begin{aligned} p \begin{bmatrix} \psi_\sigma \\ e \end{bmatrix} &= \underbrace{\begin{bmatrix} 0 & I \\ 0 & 0 \end{bmatrix}}_{\text{the homogeneous part}} \begin{bmatrix} \psi_\sigma \\ e \end{bmatrix} \\ &\quad + \underbrace{\begin{bmatrix} u_s \\ 0 \end{bmatrix} + \begin{bmatrix} -i_s & 0 & 0 \\ 0 & J e & -p i_s - L_\mu^{-1} e \end{bmatrix} \begin{bmatrix} r_s \\ \omega \\ r_{req} \end{bmatrix}}_{\text{the regressive part}} \end{aligned}$$

from which we are aware that the regressive part contains the unmeasured states e .

The observer is established as follows

$$\begin{aligned} p \hat{\psi}_\sigma &= u_s - \hat{r}_s i_s + \hat{e} + v_\sigma \\ p \hat{e} &= -\hat{r}_{req} (p i_s + L_\mu^{-1} \hat{e}) + \hat{\omega} J \hat{e} + v_\mu \end{aligned} \quad (4)$$

where v_σ and v_μ are corrective terms specified later. Define the observation errors as $\varepsilon = \psi_\sigma - \hat{\psi}_\sigma$ and $\tilde{e} = e - \hat{e}$, and the error dynamics are deduced as

$$\begin{aligned} p \varepsilon &= -v_\sigma + \tilde{e} - \tilde{r}_s i_s \\ p \tilde{e} &= -v_\mu - (\alpha I - \omega J) \tilde{e} - \tilde{r}_{req} (p i_s + L_\mu^{-1} \hat{e}) + \tilde{\omega} J \hat{e} \end{aligned} \quad (5)$$

where $\alpha = r_{req}/L_\mu$, and a tilde \sim denotes error (see nomenclature).

C. Heuristics of the Adaptive Design

Consider a virtual system whose states are denoted by $\varepsilon_{eq} = [\varepsilon_{\alpha,eq}, \varepsilon_{\beta,eq}]^T$ and $\tilde{\varepsilon}_{eq} = [\tilde{\varepsilon}_{\alpha,eq}, \tilde{\varepsilon}_{\beta,eq}]^T$, and the dynamics of ε_{eq} and $\tilde{\varepsilon}_{eq}$ are

$$\begin{aligned} p \varepsilon_{eq} &= -k \varepsilon_{eq} + \tilde{\varepsilon}_{eq} + (\tilde{r}_s w^1 + \tilde{\omega} \varphi + \tilde{r}_{req} \phi) \\ p \tilde{\varepsilon}_{eq} &= -k_2 \varepsilon_{eq} - (\alpha I - \omega J) \tilde{\varepsilon}_{eq} + c (\tilde{r}_s w^1 + \tilde{\omega} \varphi + \tilde{r}_{req} \phi) \end{aligned} \quad (6)$$

where k, k_2 and c are proper positive reals, and $w^1, \varphi, \phi \in \mathbb{R}^2$ are the regressors. Please note that (6) would be in the observable canonical form if the term $-(\alpha I - \omega J) \tilde{\varepsilon}_{eq}$ was absent, and also note that the dynamics of $\varepsilon_{\alpha,eq}$ and $\tilde{\varepsilon}_{\alpha,eq}$ (respectively, of $\varepsilon_{\beta,eq}$ and $\tilde{\varepsilon}_{\beta,eq}$) are disturbed by the same scalar disturbance $\tilde{r}_s w_\alpha^1 + \tilde{\omega} \varphi_\alpha + \tilde{r}_{req} \phi_\alpha$ (respectively, $\tilde{r}_s w_\beta^1 + \tilde{\omega} \varphi_\beta + \tilde{r}_{req} \phi_\beta$).

The stability proof of this virtual system (6) involves standard arguments of a Lyapunov function and the Kalman-Yakubovich lemma (see Appendix B), from which, recalling the assumption that $p \omega = p r_s = p r_{req} = 0$, the derived parameter adaptation rules are

$$\begin{aligned} p \hat{r}_s &= \gamma_{rs} \varepsilon_{eq}^T w^1 \\ p \hat{\omega} &= \gamma_\omega \varepsilon_{eq}^T \varphi \\ p \hat{r}_{req} &= \gamma_{rreq} \varepsilon_{eq}^T \phi \end{aligned} \quad (7)$$

where $\gamma_{rs}, \gamma_\omega$ and γ_{rreq} are positive adaptation gains.

In the sequel, the expected results are the asymptotical output-equivalence between dynamics (5) and (6), i.e., $\varepsilon \rightarrow \varepsilon_{eq}$ as $t \rightarrow \infty$, so that (7) is replaced by (8)

$$\begin{aligned} p \hat{r}_s &= \gamma_{rs} \varepsilon^T w^1 = -\dot{\tilde{r}}_s \\ p \hat{\omega} &= \gamma_\omega \varepsilon^T \varphi = -\dot{\tilde{\omega}} \\ p \hat{r}_{req} &= \gamma_{rreq} \varepsilon^T \phi = -\dot{\tilde{r}}_{req} \end{aligned} \quad (8)$$

Differentiate $p \varepsilon$ and $p \varepsilon_{eq}$ respectively, and it yields

$$\begin{aligned} p^2 \varepsilon &= -p v_\sigma - v_\mu - (\alpha I - \omega J) \tilde{e} \\ &\quad + p (-\tilde{r}_s i_s) - \tilde{r}_{req} (p i_s + L_\mu^{-1} \hat{e}) + \tilde{\omega} J \hat{e} \end{aligned} \quad (9a)$$

$$\begin{aligned} p^2 \varepsilon_{eq} &= -k p \varepsilon_{eq} - k_2 \varepsilon_{eq} - (\alpha I - \omega J) \tilde{\varepsilon}_{eq} \\ &\quad + (p + c) (\tilde{r}_s w^1 + \tilde{\omega} \varphi + \tilde{r}_{req} \phi) \end{aligned} \quad (9b)$$

where expressions of $p e$ and $p e_{eq}$ have been substituted. Now, with the design of the corrective terms

$$\begin{aligned} v_\sigma &= k \varepsilon \\ v_\mu &= k_2 \varepsilon - \dot{\tilde{r}}_s (i_s + w^1) - \dot{\tilde{\omega}} \varphi - \dot{\tilde{r}}_{req} \phi \end{aligned} \quad (10)$$

and the filtered regressors (i.e., w^1, φ and ϕ)

$$\begin{aligned} p w^1 &= -c w^1 - p i_s \\ p \varphi &= -c \varphi + J \hat{e} \\ p \phi &= -c \phi - p i_s - L_\mu^{-1} \hat{e} \end{aligned} \quad (11)$$

we subtract (9b) from (9a), and the following transfer functions are derived

$$(p^2 + kp + k_2) \Delta\varepsilon = -(\alpha I - \omega J) \Delta\tilde{e} \quad (12)$$

where $\Delta\varepsilon = \varepsilon - \varepsilon_{eq}$ and $\Delta\tilde{e} = \tilde{e} - \tilde{e}_{eq}$. If the disturbance $\Delta\tilde{e}$ is null, one concludes that the error dynamics (5) is asymptotically equivalent (in the sense of having the same outputs) to the ones (6). In other words, it concludes that the stability in the $(\varepsilon_{eq}, \tilde{e}_{eq}, \tilde{r}_s, \tilde{\omega}, \tilde{r}_{req})$ space implies the stability in the $(\varepsilon, \tilde{e}, \tilde{r}_s, \tilde{\omega}, \tilde{r}_{req})$ space [58].

With $\Delta\tilde{e} \neq 0$, $\Delta\varepsilon$ would still behave as if $\Delta\varepsilon = [0, 0]^T$ is an asymptotically stable equilibrium point when $\|\Delta\varepsilon\| > \frac{1}{k_2} \|(\alpha I - \omega J) \Delta\tilde{e}\|$. Hence, by choosing a sufficiently large k_2 , the norm of $\Delta\varepsilon$ is kept arbitrarily small with respect to the disturbance $\Delta\tilde{e}$. However, in this case, the output-equivalence between dynamics (5) and (6) cannot be established. As a result, ε_{eq} is generally an approximation of ε , as time evolves. In addition, one shall notice that this does not necessarily mean the system is unstable. Further insights into stability are desired.

Remark (an artful disposal): For the readers familiar with the work of Kudva and Narendra [58], note that the original regressor $-i_s$ (of r_s) appears only in the ε dynamics, and is absent in the \tilde{e} dynamics, thus the corresponding filtered regressor w^1 shall be driven by *the derivative of the original regressor*. (The superscript 1 indicates this difference.) It is unwanted and we should generally refrain from taking derivatives. Coincidentally, however, p_{i_s} essentially appears in the dynamics of \tilde{e} . Therefore, we've had the design.

D. Brief Summary

So far, the design of the adaptive observer is complete. The whole scheme is of order 10. The 4th order observer is proposed in (4) with the corrective terms given in (10). The 3rd order filtered regressors are given in (11). The 3rd order parameter adaptation rules are listed in (8).

The adaptive observer is dependent on L_μ , L_σ , and the initial values of r_s , ω and r_{req} ; it contains 6 design coefficients (i.e., γ_{rs} , γ_ω , γ_{rreq} , k , k_2 and c); its inputs are u_s , i_s and p_{i_s} ; its outputs are \hat{i}_s , \hat{e} , \hat{r}_s , \hat{r}_{req} and $\hat{\omega}$. A block diagram of the adaptive observer is sketched in Fig. 1. The last thing to do is to reconstruct the current derivative p_{i_s} .

E. Current Derivative Recovered by State Variable Filter

Consider the following first-order low-pass filter

$$y = \frac{p_0}{p + p_0} u \quad (13)$$

where $-p_0$ is the pole of the filter. If the cut-off frequency of the filter is high enough such that the output y ‘coincides with’ the input u , the derivative of u can then be approximately recovered (see Fig. 1). Such a filter is called *state variable filter* (SVF) [13], [17], by means of which p_{i_s} may be recovered without resorting to pure differentiation.

By intuition, the selection of the value of p_0 should be a compromise between the sensitivity to stator current noises and the accuracy of derivative approximation. If a large p_0 is

TABLE II. Coefficients Adopted in the Paper

Observer Coefficients	Notation	Values
Correction gain to ε	k	355 s^{-1}
Correction gain to \tilde{e}	k_2	1580 s^{-2}
The pole of the regressor filters	$-c$	-3 s^{-1}
The pole of state variable filter	$-p_0$	$-800 \times 2\pi \text{ s}^{-1}$
Adaptation gain of speed	γ_ω	$5.2\text{e}4 \text{ rad}/(\text{s}^2\text{Wb}^2)$
Adapt. gain of stator resistance	γ_{rs}	$200 (\text{sAWb})^{-1}$
Adapt. gain of rotor resistance	γ_{rreq}	$1200 (\text{sAWb})^{-1}$
Controller Coefficients	Notation	Values
The DC part of the flux modulus	m_0	0.6 Wb
Frequency of the sinusoidal part	ω_1	1 Hz
Amplitude of the sinusoidal part	m_1	0.1 Wb
Proportional gain of speed regulator	$K_{P\omega}$	$0.5 \text{ A}(\text{rad/s})^{-1}$
Integral time constant of speed regulator	$T_{I\omega}$	0.1 rad/A

used, the output of the SVF will be highly noisy. Fortunately, as long as the noises are of zero-mean, the mean values of estimated parameters still converge, indeed. On the other hand, if p_0 is too small so that the output of the SVF is delayed with respect to the actual current derivative, the identification of parameters will then be biased, especially for that of stator resistance. In conclusion, a relatively large p_0 should be chosen.

III. THE WHOLE SYSTEM

The above adaptive observer offers $\hat{\omega}$, \hat{r}_{req} , and \hat{e} . To be specific, \hat{r}_{req} is crucial for the feed-forward field orientation and the flux modulus estimator, $\hat{\omega}$ is used for sensorless speed control, and \hat{e} comes in handy when designing decoupling circuits for current regulation.

A. The Indirect Field Oriented Control (FOC)

1) *Flux modulus control:* For parameter identification purpose, the biased sinusoidal flux modulus command

$$|\psi_\mu^*| = m_0 + m_1 \sin(\omega_1 t) \quad (14)$$

is required to distinguish between speed ω and rotor resistance r_{req} , where the numerical values of m_0 , m_1 and ω_1 are given in Table II. The magnetizing current command i_{Ms}^* follows as

$$i_{Ms}^* = \frac{1}{\hat{r}_{req}} |\dot{\psi}_\mu^*| + \frac{1}{L_\mu} |\psi_\mu^*.| \quad (15)$$

2) *Speed control:* The speed control is realized by a proportional-integral regulator as follows

$$i_{Ts}^* = -K_{P\omega} \left(1 + \frac{1}{T_{I\omega} p} \right) (\hat{\omega} - \omega^*) \quad (16)$$

where $K_{P\omega}$ and $T_{I\omega}$ are positive constants.

3) *Feed-forward field orientation:* The commanded rotor flux angle ρ^* indicates the location of the M -axis of the $M-T$ frame, and it is determined in a feed-forward fashion

$$p\rho^* = \omega_\psi^* \triangleq \hat{\omega} + \omega_{sl}^* \quad (17)$$

where ω_ψ^* denotes the commanded synchronous speed, and the slip angular speed is $\omega_{sl}^* = \hat{r}_{req} i_{Ts}^*/|\psi_\mu^*|$.

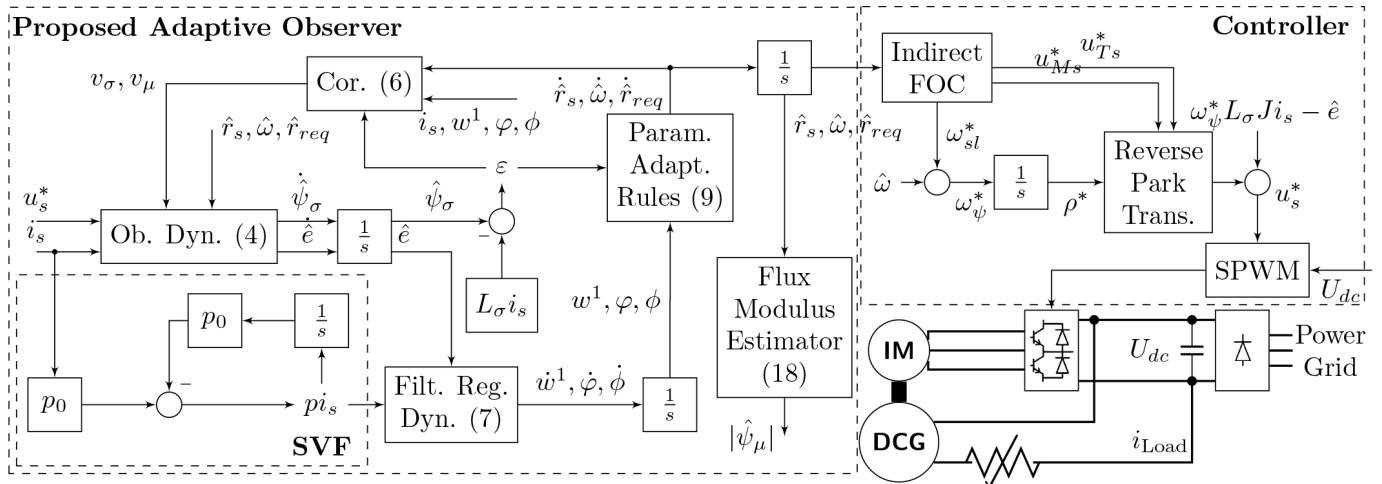


Fig. 1. Block diagram of the proposed system. (Filt. Reg. Dyn.: Filtered Regressor Dynamics. Ob. Dyn.: Observer Dynamics. Cor.: Corrective terms.)

B. Flux Modulus Estimator

Since the angle of the rotor flux has been determined in a feed-forward fashion, a flux observer seems now redundant, so a flux modulus estimator shall suffice [59], [37], i.e.,

$$p |\hat{\psi}_\mu| = -\frac{\hat{r}_{req}}{L_\mu} |\hat{\psi}_\mu| + \hat{r}_{req} i_{Ms} \quad (18)$$

where $i_{Ms} = \cos(\rho^*) i_{\alpha s} + \sin(\rho^*) i_{\beta s}$ is the stator magnetizing current. In fact, the estimator (18) is robust to speed uncertainty, so it will remain undisturbed during speed transient when speed estimated error is large.

C. Decoupling Circuits for Current Regulation

As stated in Vas [60], in the synchronous rotating $M-T$ frame, there are rotational voltage coupling terms in either M -axis or T -axis voltage equation

$$\begin{aligned} u_{Ms} &= r_s i_{Ms} + L_\sigma p i_{Ms} + \underbrace{p \psi_{M\mu} - \omega_\psi (L_\sigma i_{Ts} + \psi_{T\mu})}_{\text{coupling terms}} \\ u_{Ts} &= r_s i_{Ts} + L_\sigma p i_{Ts} + \underbrace{p \psi_{T\mu} + \omega_\psi (L_\sigma i_{Ms} + \psi_{M\mu})}_{\text{coupling terms}} \end{aligned} \quad (19)$$

As a result, the T -axis stator current i_{Ts} affects the M -axis stator voltage u_{Ms} , and vice versa. Assuming that $\psi_{T\mu} = 0$ and $\psi_{M\mu} = L_\mu i_{Ms}$, a steady-state equation based decoupling circuits is designed in [60, Sec. 4.1.1.3] (see also [33], [61]). Besides, a dynamic equation based decoupling circuits can be constructed as well, provided that $\hat{\psi}_\mu$, $\hat{\alpha}$ and $\hat{\omega}$ are available [62].

Particularly, in this paper, with the back electromotive force e estimated by the observer (4), we are able to cancel the coupling terms directly in the $\alpha-\beta$ frame as follows (shown in the controller area of Fig. 1)

$$u_s^* = \begin{bmatrix} \cos \rho^* & -\sin \rho^* \\ \sin \rho^* & \cos \rho^* \end{bmatrix} \begin{bmatrix} u_{Ms}^* \\ u_{Ts}^* \end{bmatrix} + \omega_\psi^* L_\sigma J i_s - \hat{e} \quad (20)$$

D. Experiment Results

1) *System Setup:* The induction motor, whose nameplate data are 4 kW, 1440 rpm, 380 V and 8.8 A, is driven by a voltage-source inverter. The load torque is provided by a separately excited DC generator. The numerical values of the tested motor and the design coefficients determined by simulated trial-and-error studies are listed in Table I and Table II respectively.

2) *Resistances Identification in Speed Sensorless IM Drives:* Fig. 2 shows the parameter identification results at 80 r/min (about 2.7 Hz excitation), and the profiles of $|\psi^*_\mu|$, $|\hat{\psi}_\mu|$, \hat{r}_s , \hat{r}_{req} , $\hat{\omega}$, $\tilde{\omega}$, $i_{\alpha s}$ and $p i_{\alpha s}$ are presented. Resistances are intentionally detuned to verify the system robustness with respect to uncertainty in resistances. Although the waveform of $p i_{\alpha s}$ is noisy owing to the slotting of the test motor, the parameter estimation stays unbiased ultimately. Furthermore, we observe that the overestimation of resistances has more severe impact on the speed sensorless control than the under-estimation case. However, because the convergent transient of resistances is short (less than 3 sec), the system is stabilized before it goes into oscillations. In addition, the low frequency part (1 Hz) of the speed ripples observed at speed steady state, is caused by the time-varying flux modulus command.

IV. STABILITY IMPROVEMENT IN REGENERATION MODE

Since the adaptive design in Sec. II-C has the defect that the output equivalence is disturbed by $\Delta \tilde{e}$, the proposed adaptive observer may become unstable with some working conditions (e.g., regeneration mode). In this section, the (absolute) stability and the relative stability of the proposed adaptive observer are evaluated by numerically computing the eigenvalues of the homogeneous matrix A_0 of the steady-state linearized model (A.1) (see Appendix A).⁷ Owing to the need of a time-varying flux modulus, the stability analysis of the r_{req} estimation is

⁷According to the Abel-Ruffini theorem, the algebraic solution of eigenvalues of A_0 , which helps to select coefficients, may not exist. Instead, the Routh-Hurwitz criterion can be applied for an analytic solution, but the coefficients in the Routh array are too involved so that it seems impossible to help.

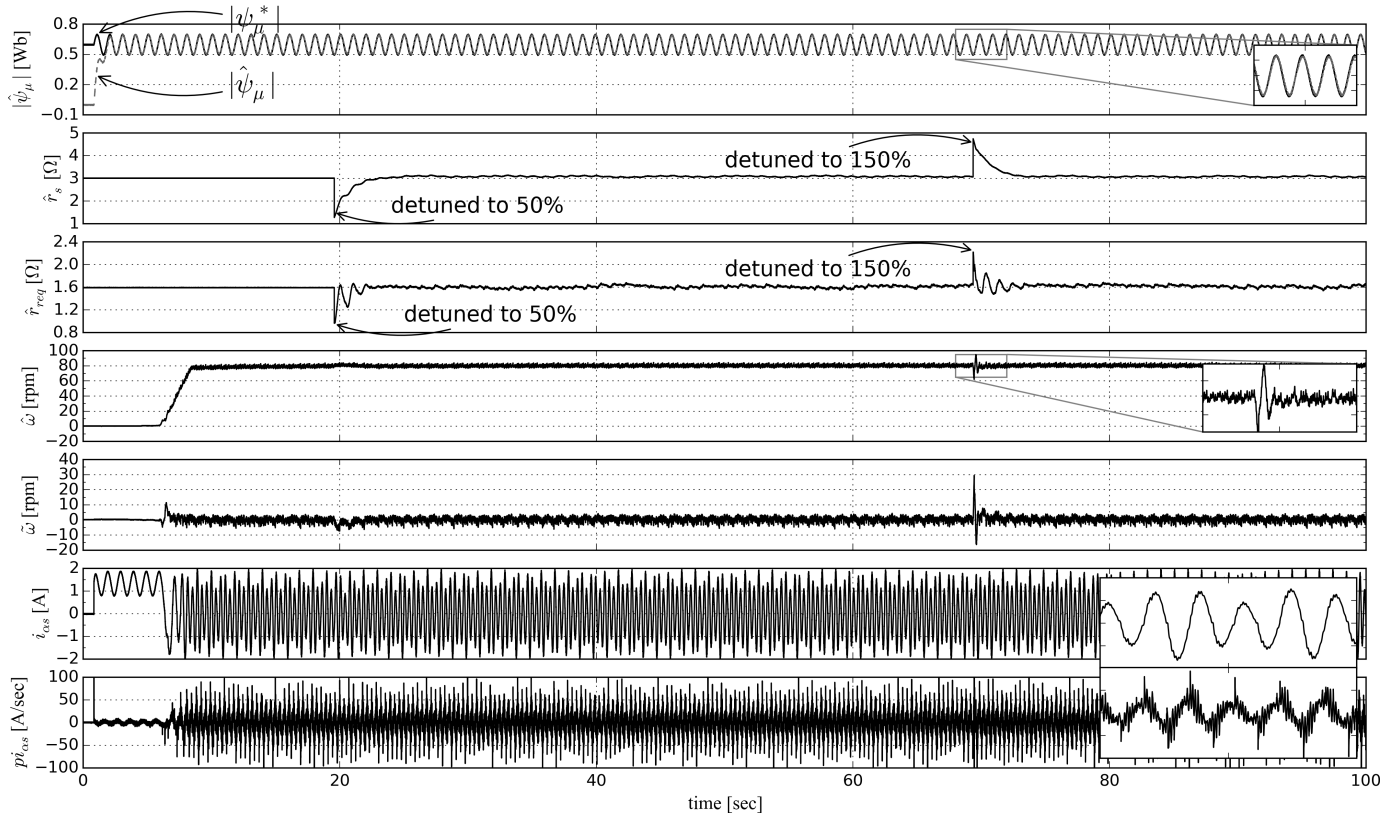


Fig. 2. Experimental speed-sensorless control using $\hat{\omega}$ and identification of r_s and r_{req} at 80 r/min. Resistances are firstly detuned to 50% at $t = 19$ sec, then detuned to 150% at $t = 69$ sec.

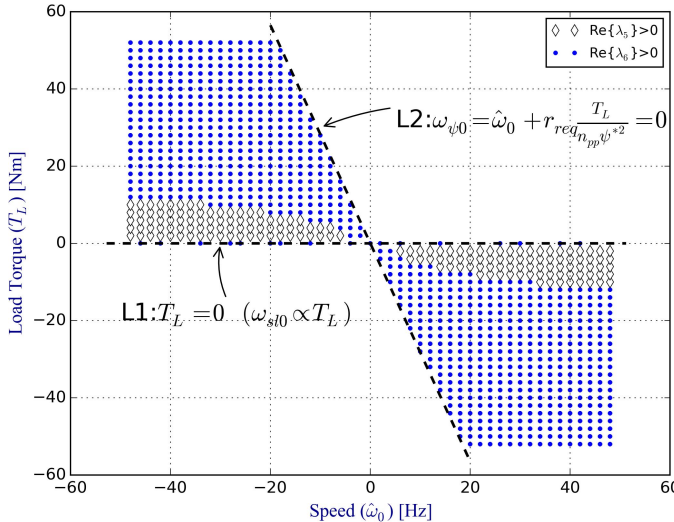


Fig. 3. Unstable regions of joint r_s & ω estimation in the $\hat{\omega}_0$ - T_L plane: the unstable eigenvalues of A_0 with respect to different working conditions are marked. Coefficients are (in SI units): $k = 355$, $k_2 = 1580$, $c = 3$, $\gamma_\omega = 100$, $\gamma_{rs} = 2$.

not included here, while a supplementary stability verification is provided instead in Appendix C.

A. Stability of Joint ω & r_s Estimation

Denote the eigenvalues of A_0 by λ_i , $i = 1, 2, \dots, 6$. In Fig. 3, the unstable regions of the joint estimation of ω and r_s are

marked over the $\hat{\omega}_0$ - T_L plane, where the subscript 0 denotes steady-state quantity. It is observed that r_s identification can be incorporated to improve speed estimation accuracy during motoring operation and plugging operation (i.e., $\omega_{sl}\omega < 0$ and $|\omega_{sl}| > |\omega|$). Please note that the instability is due to $\text{Re}\{\lambda_5\} > 0$ or $\text{Re}\{\lambda_6\} > 0$. That is, λ_5 and λ_6 are not going to be unstable for the same operating point.

One can compute the determinate of A_0 as

$$\det A_0 = \prod_{i=1}^6 \lambda_i = \frac{2\gamma_\omega \gamma_{rs} i_{Ms0}^2 |\psi_\mu^*|^2}{c^2 + \omega_{\psi0}^2} \omega_{\psi0}^3 \omega_{sl0} \quad (21)$$

According to Etien *et al.* [39], if the instability is due to one single right-half-plane (RHP) eigenvalue, (which is true for the case of r_s and ω joint estimation,) then the boundaries between stable regions and unstable regions can be predicted by the solutions of $\det A_0 = 0$, i.e., $\omega_{sl0} = 0$ (denoted by L1) and $\omega_{\psi0} = 0$ (denoted by L2). However, from (21), it is apparently impossible to reduce the unstable region in the regeneration mode by selecting design coefficients of c , k , k_2 , γ_ω and γ_{rs} . As a result, the estimation of r_s should be avoided during regenerating operation.

B. Stability of ω Estimation

With the estimation of r_s suspended (i.e., $\gamma_{rs} = 0$), the stability of ω estimation is analyzed by evaluating the eigenvalues of the 5×5 sub-matrix $\det A_{0,5}$ [see (A.4)].

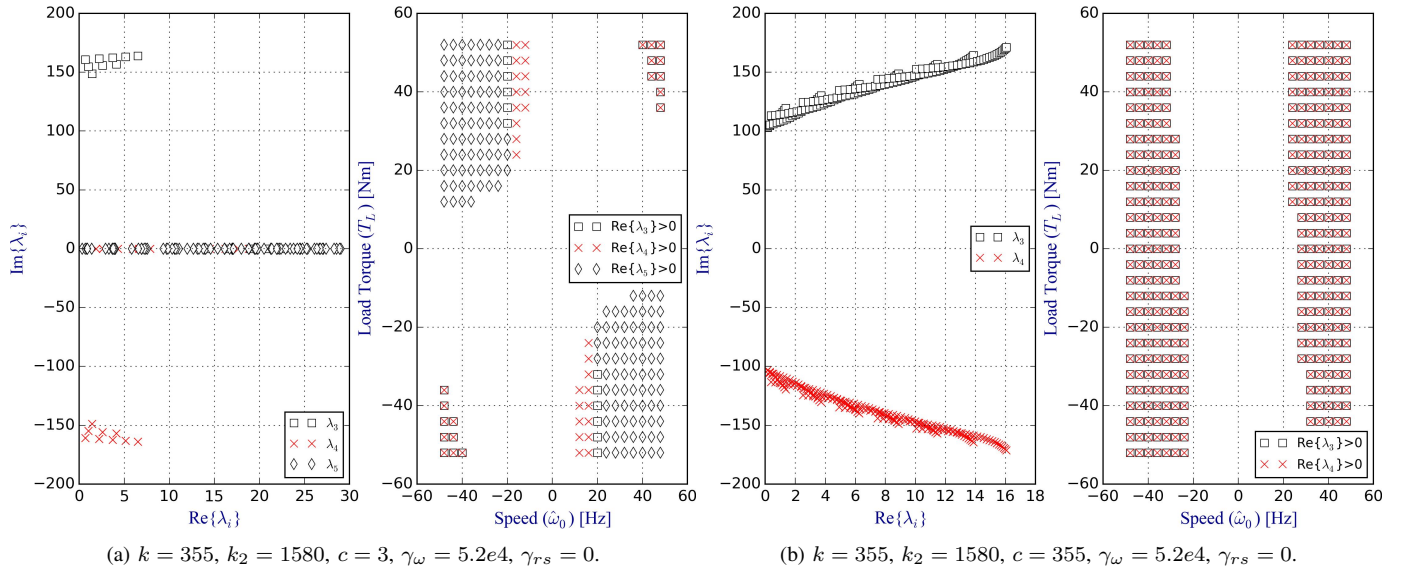


Fig. 4. Scatter plot of unstable eigenvalues of $A_{0,5}$ in the $\text{Re}\{\lambda_i\}$ - $\text{Im}\{\lambda_i\}$ plane and the $\hat{\omega}_0$ - T_L plane.

One computes

$$\det A_{0,5} = \left(\frac{\gamma_\omega \omega_{\psi 0}^2 |\psi_\mu^*|^2}{c^6 + 3c^4 \omega_{\psi 0}^2 + 3c^2 \omega_{\psi 0}^4 + \omega_{\psi 0}^6} \right) \times \begin{cases} -\alpha \omega_{\psi 0}^6 + \omega_{\psi 0}^5 (c \omega_{sl0} - k \omega_{sl0}) \\ + \omega_{\psi 0}^4 (-2\alpha c^2 - \alpha c k - 2c \gamma_\omega |\psi_\mu^*|^2 - ck_2) \\ + \omega_{\psi 0}^3 (2c^3 \omega_{sl0} - 2c^2 k \omega_{sl0}) \\ + \omega_{\psi 0}^2 (-\alpha c^4 - 2\alpha c^3 k - 2c^3 k_2) \\ + \omega_{\psi 0} (c^5 \omega_{sl0} - c^4 k \omega_{sl0}) - \alpha c^5 k - c^5 k_2 \end{cases} \quad (22)$$

from which we observe that if we let $c = k$, the odd-order power terms of $\omega_{\psi 0}$ will disappear. In fact, such selection of design coefficients cancels all the *real* RHP eigenvalues of $A_{0,5}$. To see this, an illustrative example follows. In Fig. 4, the RHP eigenvalues of $A_{0,5}$ are marked in the $\text{Re}\{\lambda_i\}$ - $\text{Im}\{\lambda_i\}$ plane as well as in the $\hat{\omega}_0$ - T_L plane. When $c \ll k$ (Fig. 4a), there are unstable eigenvalues on the real-axis, but when $c = k$ (Fig. 4b), unstable eigenvalues appear only in conjugate pairs.

Unfortunately, we cannot get more design hints by continuing to simplify $\det A_{0,5}$ until $\det A_{0,5} \propto \omega_{\psi}^2$, because the sign of $\det A_{0,5}$ stays unchanged when a pair of conjugate eigenvalues becomes either stable or unstable. Even though, based on our research, we suggest the selection of design coefficients to satisfy

$$\text{Design A : } \begin{cases} c \geq 0.05 \gamma_\omega > 0 \\ k \approx c \\ k_2 \neq 0 \end{cases} \quad (23)$$

which is found to generally stabilize the proposed speed adaptive observer during regenerating operation, including zero-frequency operation. For instance, consider the coefficients selection (in SI units): $c = k = 355$, $k_2 = 1580$, $\gamma_\omega = 7100$, $\gamma_{rs} = 0$, and it will stabilize the linearized model all over the $\hat{\omega}_0$ - T_L plane except the origin $(\hat{\omega}_0, T_L) = (0, 0)$ (see Fig. 5a). In other words, those RHP eigenvalues in conjugate pairs

marked in Fig. 4b are removed, by decreasing the values of γ_ω .

Remark: As a comparison, in regenerative mode, the speed adaptive full-order observer can be stabilized by assigning proper feedback gains and adaptation laws, which, however, may be dependent on the actual speed [39]. This is unrealistic. Still, zero-frequency operation is not assured therein.

C. Practical Stability of ω Estimation

The observer with Design A (23) works fine in simulation with perfect knowledge of motor parameters and small speed estimation error. However, as shown in Fig. 5a, since λ_5 becomes near the imaginary-axis during regeneration mode, the speed estimation error converges so slow that the instability phenomenon called ‘flux collapse’ [31] usually occurs when the speed estimation error becomes large. Thus, Design A (23) is not robust enough for practical application.

Based on our research, we give here a distinct stable design of practical significance:

$$\text{Design B : } \begin{cases} c = |\omega_{\psi}^* \hat{\omega}| / \alpha; \\ k_2 \text{ is large enough, e.g., } k_2 > 5500; \\ \gamma_\omega \propto k_2, \text{e.g., } \gamma_\omega \approx 10k_2; \\ k = 2 \times \text{damping_ratio} \times \omega_{\text{Natural}} \\ \text{with damping_ratio} = 0.707, \\ \text{and } \omega_{\text{Natural}} = \sqrt{k_2}. \end{cases} \quad (24)$$

Firstly, a time-varying c is adopted, i.e., $c = |\omega_{\psi}^* \hat{\omega}| / \alpha$, where the factor $\frac{1}{\alpha}$ is an optimal choice in the sense of the nicer performance of speed estimation and the larger stability margin. This choice of c is due to Etien *et al.* [39], but differs for the absolute value.

Secondly, if $c \propto |\omega_{\psi}^* \hat{\omega}|$, then a large value of k_2 essentially stabilizes the adaptive observer, which is a natural choice, because it is already suggested in Sec. II-C that a large value of k_2 facilitates the stability in the sense of Lyapunov. (It is,

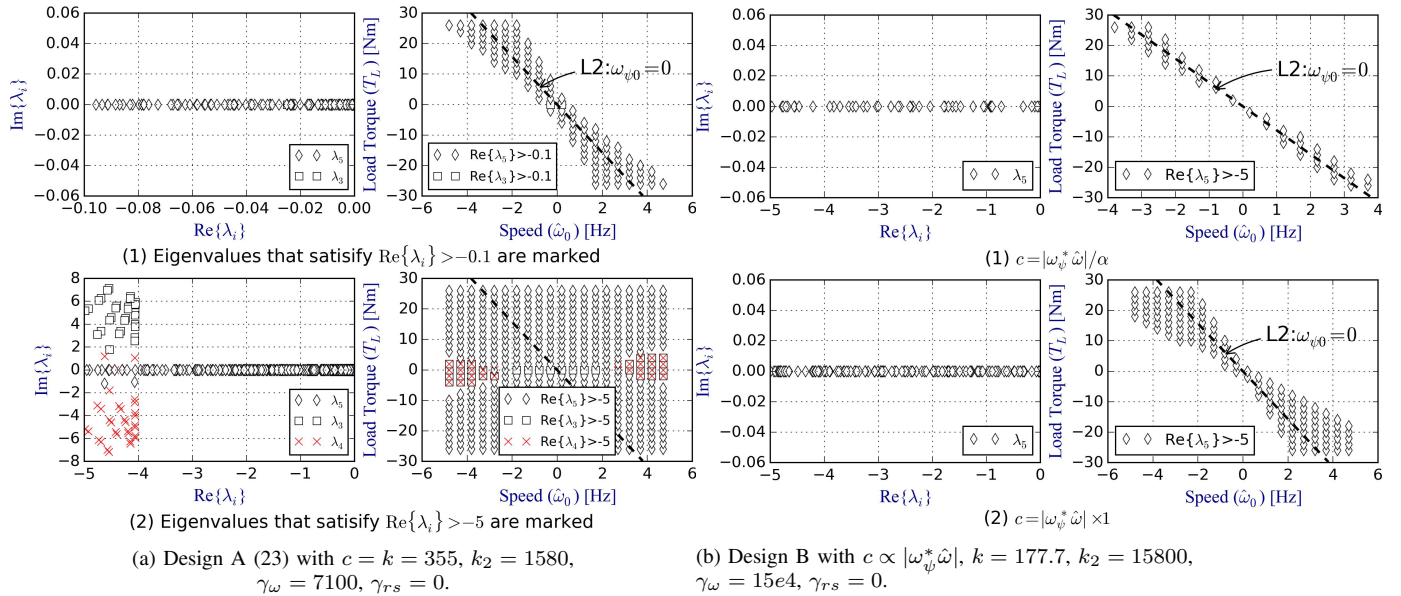


Fig. 5. Illustration of stability margin of $A_{0,5}$ in low speed region. (a) Design A—the real parts of all the dominant eigenvalues are larger than -5 , and they become even larger near L2 (larger than -0.1). (b) Design B—the real parts of all the dominant eigenvalues away from the vicinity of L2 are less than -5 , and the optimal factor $1/\alpha$ results in larger stability margin.

however, interesting to point out that k_2 has little influence on the stability when c is fixed to a constant.)

Thirdly, since k_2 determines the sensitivity of ε with respect to $\hat{\omega}$, it should be tuned together with γ_ω . That is, the larger k_2 , the larger γ_ω , so the dynamic performance of speed estimation is assured. Finally, the value of k is selected to obtain proper damping of the second-order transfer functions (12).

Design B is preferred over Design A, though they are both stable designs. To see this, we shall study the relative stability. That is, the eigenvalues of $A_{0,5}$ whose real parts are larger than -0.1 or -5 are marked in both the $\text{Re}\{\lambda_i\}$ - $\text{Im}\{\lambda_i\}$ plane and the $\hat{\omega}_0$ - T_L plane in Fig. 5.

Remark: As is suggested by Etien *et al.* [39], in order to obtain a robust and stable speed estimation without resistance identification, one should resort to an appropriate redesign of the speed adaptation law—in our case an appropriate design of c (cf. the discussion in Sec. V-A).

D. Experiment Results

1) *Sensored Speed-Torque Characteristic:* In Fig. 6a, presented are the waveforms of speed, i_{Ts} , T_L , ρ^* and current during the sensored control experiment. The tested motor undergoes (in order) motoring operation, slow reversal, plugging operation, zero-frequency operation, and finally regenerating operation. The shaded time-span (from 168 sec to 176 sec), when the load is being removed, shows the unstable estimation near the zero-frequency excitation. Based on the data of Fig. 6a, the speed-torque characteristic is plotted in Fig. 6b. One concludes that the stability of the speed estimation is preserved during both motoring and regeneration modes, except zero-frequency operation.

The speed ripples are mainly caused by rotor slot harmonics (RSHs) whose influence is amplified as the load gets heavy. The Fourier analysis of the speed (see Fig. 7a) shows the

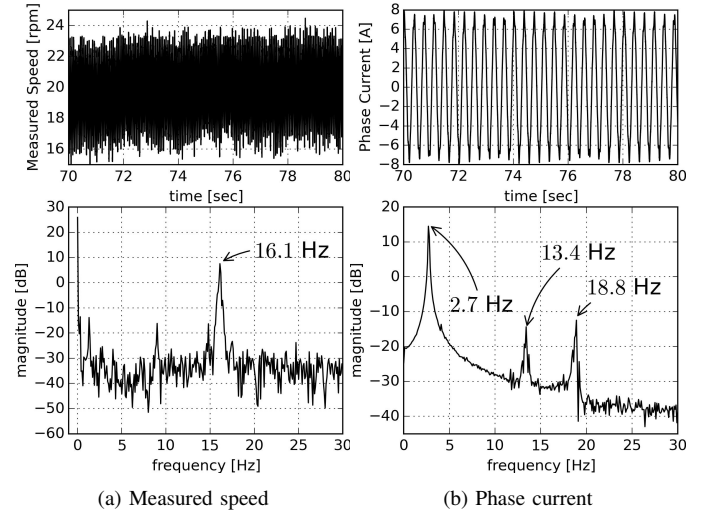


Fig. 7. Fourier analysis of signals from Fig. 6 between 70 sec and 80 sec.

frequency of the harmonic in speed is 16.1 Hz. Owing to the modulation of the electromagnetic fields [63], the 16.1 Hz harmonic in speed corresponds to the $-13.4 (= 2.7 - 16.1)$ Hz and the 18.8 ($= 2.7 + 16.1$) Hz harmonics in current, which is confirmed by the Fourier analysis of current (see Fig. 7b).⁸

2) *Sensorless Fast Reversal Test:* In Fig. 8, presented are the experiment results of the sensorless speed reversing test between -20 r/min and 20 r/min, which concludes that

⁸The frequency of the dominant RSH of the tested motor is [6]

$$f_{DH} = -\frac{1}{2\pi} \left(\frac{Z_r}{n_{pp}} \omega + \omega_\psi \right) \approx -\left(\frac{32}{2} \times 0.67 + 2.7 \right) \text{ Hz} = -13.42 \text{ Hz} \quad (25)$$

where $Z_r = 32$ is the number of rotor slots, $\frac{\omega}{2\pi} = 0.67$ Hz, and $\frac{\omega_\psi}{2\pi} = 2.7$ Hz.

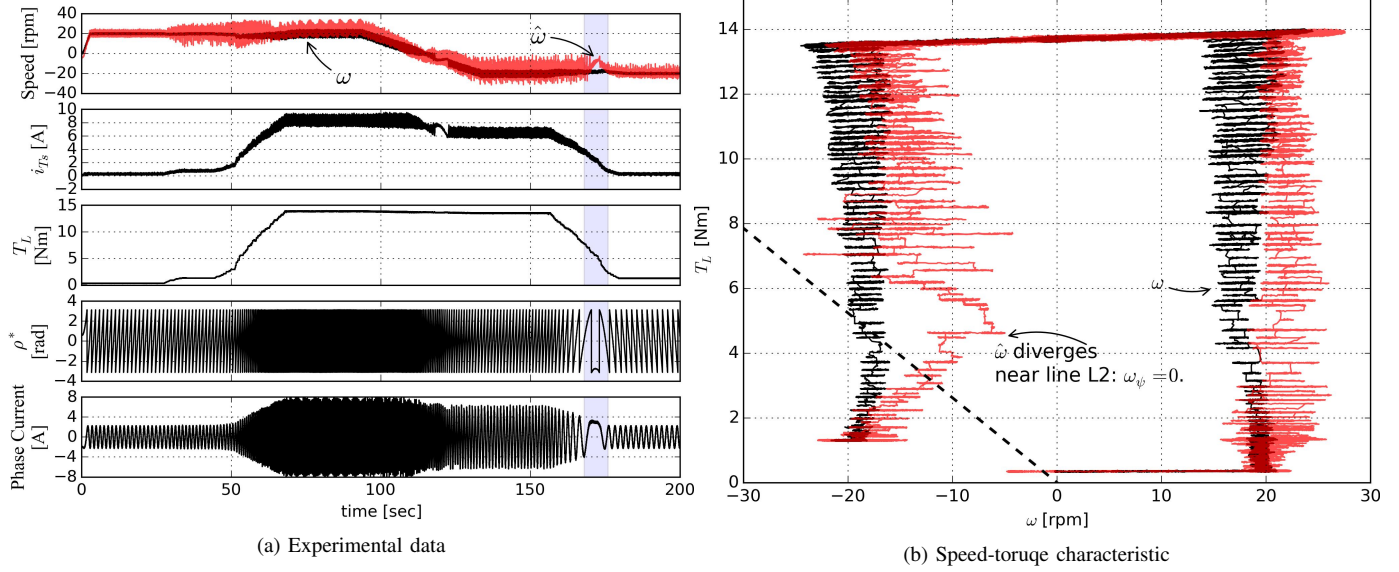


Fig. 6. Speed-torque characteristic obtained by sensed control. The proposed observer is implemented with Design B and $\hat{\omega}$ is not used for control.

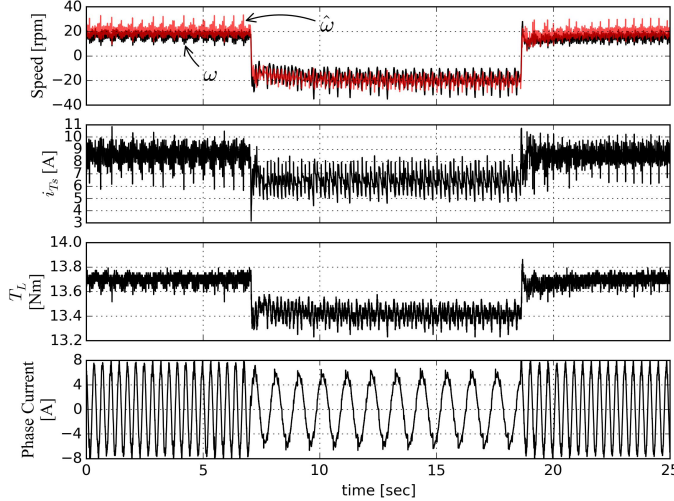


Fig. 8. Sensorless fast reversal test under load with Design B.

the sensorless control with the proposed adaptive observer can operate at both motoring mode (i.e., $\omega_{iTs} > 0$) and regeneration mode (i.e., $\omega_{iTs} < 0$).

3) Sensorless Slow Reversal Test: In Fig. 9, the experiment results of the sensorless slow reversal test are given. From $t = 0$ sec to $t = 60$ sec, although the speed ripples are apparent, the speed varies from 20 rpm to -20 rpm stably with $T_L \approx 14$ Nm.

The shaded time-span (from 61 sec to 77 sec), when the load is being removed, shows the unstable behavior near the zero-frequency excitation. It is observed that the instability occurs before the stator frequency equals to zero. This is because the speed perturbation makes the operating point move across the zero-frequency line (L2), which enlarges the unstable operating region. We conclude that, in extreme circumstances, the practical stability margin of the system should be carefully checked.

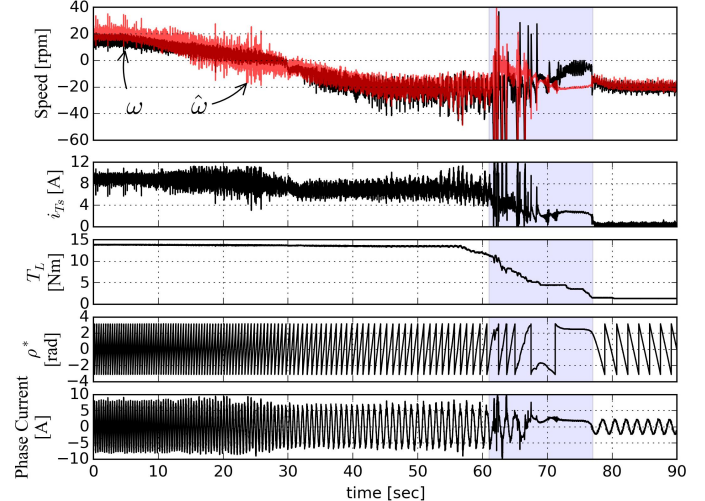


Fig. 9. Sensorless slow reversal test under load with Design B. The unstable zero-frequency crossing is highlighted by the transparent shadow.

V. DISCUSSION

A. The Relation to the Method of Hinkkanen & Luomi [40]

In [40], instead of using only the current estimated error perpendicular to the estimated flux, the parallel component is also exploited in the regeneration mode, that is,

$$\hat{\omega} = -\gamma_P \epsilon - \gamma_I \int \epsilon dt \quad (26)$$

$$\text{with } \epsilon = |\hat{\psi}_\mu| \left[(i_{Ts} - \hat{i}_{Ts}) \cos \phi_c - (i_{Ms} - \hat{i}_{Ms}) \sin \phi_c \right]$$

where ϕ_c is a scalar to be designed, and $\gamma_P, \gamma_I \in \mathbb{R}$. The conventional choice is $\phi_c = 0$.

The proposed speed adaptation law in (8) can be rewritten

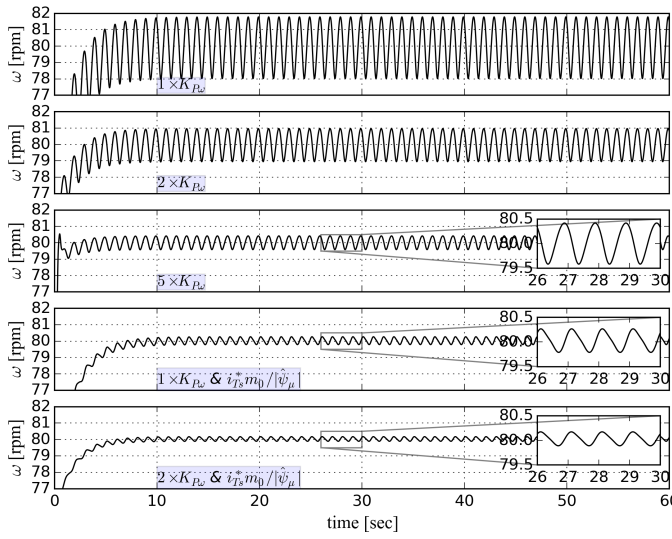


Fig. 10. Simulation results of reduction of speed ripples caused by time-varying flux modulus command (sensorless control is implemented). From top to bottom are respectively the cases of (in SI units) $K_{P\omega} = 0.5$, $K_{P\omega} = 1$, $K_{P\omega} = 2.5$, $K_{P\omega} = 0.5$ & $i_{Ts}^* \frac{m_0}{|\psi_\mu|}$, and finally $K_{P\omega} = 1$ & $i_{Ts}^* \frac{m_0}{|\psi_\mu|}$.

with components in $M-T$ frame as

$$\begin{aligned} p\hat{\omega} &= \gamma_\omega \begin{bmatrix} \varepsilon_\alpha & \varepsilon_\beta \end{bmatrix} \begin{bmatrix} \varphi_\alpha \\ \varphi_\beta \end{bmatrix} = \gamma_\omega \left(T \begin{bmatrix} \varepsilon_\alpha \\ \varepsilon_\beta \end{bmatrix} \right)^T T \begin{bmatrix} \varphi_\alpha \\ \varphi_\beta \end{bmatrix} \\ &= \gamma_\omega (\varepsilon_M \varphi_M + \varepsilon_T \varphi_T) \end{aligned} \quad (27)$$

where $T = \begin{bmatrix} \cos \rho^* & \sin \rho^* \\ -\sin \rho^* & \cos \rho^* \end{bmatrix}$, and note that $T^T T = I$. In steady state, law (27) is an equivalent implementation of (26) with $\gamma_P = 0$, if we select c to satisfy

$$\begin{aligned} \frac{\varphi_{M0}}{\varphi_{T0}} &= \frac{c\omega_\psi}{-\omega_\psi^2} \propto \frac{-\sin \phi_c}{\cos \phi_c} \\ &\Rightarrow c \propto \omega_\psi \tan \phi_c \end{aligned} \quad (28)$$

where φ_{M0} and φ_{T0} are listed in (A.3). In [39], it is suggested that $\tan \phi_c = \omega/\alpha$, which is equivalent (in steady state) to implement $c \propto \omega_\psi \omega/\alpha$.

B. Reduction of Speed Ripples

There are two effective ways to alleviate the speed ripples that are due to time-varying flux modulus. The first one is to increase the proportional gain $K_{P\omega}$ of speed control, which also expedites the speed transient. While the other is to incorporate exact input-output linearizing control, e.g., simply multiplying i_{Ts}^* obtained from (16) by $\frac{m_0}{|\psi_\mu|}$. To illustrate both the statements, we give results of several situations in Fig. 10.

From Fig. 10, we notice that the speed ripples are only reduced rather than eliminated, and this may be explained by the fact that the proportional-integral regulators (of currents) should not be expected to track the time-varying commands i_{Ms}^* and $i_{Ts}^* \frac{m_0}{|\psi_\mu|}$.

Remark: In contrast, the scheme proposed in [45] needs to intentionally disturb the speed so as to detect the sign of the T -axis flux estimated error from the resulting i_{Ts}^* . Such speed disturbance cannot be compensated or cancelled.

C. Further Identification of L_μ

Replace L_μ with \hat{L}_μ so that $\hat{\alpha} = \hat{r}_{req} \hat{L}_\mu^{-1}$. And noticing that

$$\begin{aligned} \tilde{\alpha} &= r_{req} L_\mu^{-1} - \hat{r}_{req} \hat{L}_\mu^{-1} \\ &= L_\mu^{-1} \tilde{r}_{req} - \hat{\alpha} L_\mu^{-1} \hat{L}_\mu \end{aligned} \quad (29)$$

the error dynamics also considering uncertainty in L_μ are rewritten in matrix form as

$$\begin{aligned} p \begin{bmatrix} \varepsilon \\ \tilde{e} \end{bmatrix} &= \begin{bmatrix} -k & I \\ -k_2 & -\alpha I + \omega J \end{bmatrix} \begin{bmatrix} \tilde{\psi}_\sigma \\ \tilde{e} \end{bmatrix} \\ &+ \begin{bmatrix} -i_s & 0 & 0 & 0 \\ 0 & -pi_s - L_\mu^{-1} \hat{e} & \hat{\alpha} L_\mu^{-1} \hat{e} & J \hat{e} \end{bmatrix} \begin{bmatrix} \tilde{r}_s \\ \tilde{r}_{req} \\ \hat{L}_\mu \\ \tilde{\omega} \end{bmatrix} \\ &+ \begin{bmatrix} 0 \\ -\dot{r}_s (i_s + w^1) - \dot{\tilde{\omega}} \varphi - \dot{\tilde{r}}_{req} \phi - \dot{\tilde{L}}_\mu \ell \end{bmatrix} \end{aligned}$$

where we have substituted for v_σ and v_μ , and ℓ is the filtered regressor for L_μ . The consequent adaptation rule for \hat{L}_μ is

$$\begin{aligned} p\hat{L}_\mu &= \gamma_{L\mu} \varepsilon^T \ell \\ p\ell &= -cl + \hat{\alpha} \hat{e} \end{aligned}$$

where the unknown constant L_μ^{-1} from the original regressor $\hat{\alpha} L_\mu^{-1} \hat{e}$ has been absorbed into the constant gain $\gamma_{L\mu}$.

D. Elimination of Current Derivative

The requirement of current derivative may be eliminated by choosing the unmeasured state as

$$\zeta = r_{req} i_s + e = r_{req} i_s - p\psi_\mu$$

In fact, the new dynamics follow as

$$\begin{cases} p\psi_\sigma = u_s - (r_s + r_{req}) i_s + \zeta \\ p\zeta = -\alpha (\zeta - r_{req} i_s) + \omega J (\zeta - r_{req} i_s) \end{cases}$$

which, however, in turn leads to the problem of over-parametrization. That is, the model is over-parameterized by αr_{req} and ωr_{req} . Still, this model is not transformable into the *adaptive observer form* because the regressive part contains ζ .

VI. CONCLUSION

The speed sensorless control of IMs with stator and rotor resistances identification is challenging. A review on 12 different solutions to the topic is given and each solution has its own shortcomings. Particularly, the last solution (method xii) has the potential to attack the topic in an elegant way, but the identification of stator resistance hinders it.

To get out of the dilemma, we explore a new direction by asking: “Is there a different representation of the IM dynamics (the electrical part) that can be transformed into the *adaptive observer form*?” Although the answer to the question still remains open, there does exist at least one representation that is ‘almost’ transformable into the *adaptive observer form*, i.e., the IM dynamics with the electromotive force as the unmeasured states. With the new representation, an adaptive observer is designed, and only current estimated error is needed for parameter adaptation.

As a flaw of the new representation, the inconformity from the class of systems that can be transformed into the *adaptive observer form* incurs a problem. In fact, the system becomes unstable during low-speed regeneration mode. Stabilization remedies that are based on stability analysis of the steady-state linearized model are provided. Effective experiment results are included, which show that the stability of the sensorless system under various circumstances can be preserved, and the convergent transient of resistances can be made fast so that system robustness is enhanced.

At last, the speed ripples problem caused by the time-varying flux modulus, the further inclusion of magnetizing inductance identification, and the removal of the current derivative requirement are discussed.

APPENDIX A STEADY-STATE LINEARIZED MODEL

We use subscript $_0$ to designate the quantity at the operating point, and use δ to indicate variation from the operating point. Define

$$\begin{aligned} x &= [\varepsilon_M \quad \varepsilon_T \quad \tilde{e}_M \quad \tilde{e}_T \quad \tilde{\omega} \quad \tilde{r}_s]^T \\ u &= [\omega_\psi \quad \omega]^T \end{aligned} \quad (\text{A.1})$$

Then, the steady-state linearized error model of the proposed observer with r_s and ω adaptation in the synchronous M - T frame can be derived as

$$p(\delta x) = A_0 \delta x + B_0 \delta u \quad (\text{A.2})$$

with $A_0 =$

$$\begin{bmatrix} -k & \omega_{\psi 0} & 1 & 0 & 0 & -i_{Ms0} \\ -\omega_{\psi 0} & -k & 0 & 1 & 0 & -i_{Ts0} \\ v_1 - k_2 & v_2 & -\alpha & \omega_{sl0} & -\hat{e}_{T0} & 0 \\ v_3 & v_4 - k_2 & -\omega_{sl0} & -\alpha & \hat{e}_{M0} & 0 \\ -\gamma_\omega \varphi_{M0} & -\gamma_\omega \varphi_{T0} & 0 & 0 & 0 & 0 \\ -\gamma_{rs} w_{M0} & -\gamma_{rs} w_{T0} & 0 & 0 & 0 & 0 \end{bmatrix}$$

and

$$B_0 = \begin{bmatrix} \varepsilon_{T0} & 0 \\ -\varepsilon_{M0} & 0 \\ \tilde{e}_{T0} & -\tilde{\psi}_{T\mu 0} \\ -\tilde{e}_{M0} & \tilde{\psi}_{M\mu 0} \\ 0 & 0 \\ 0 & 0 \end{bmatrix}$$

where the 2×2 block matrix is

$$\begin{bmatrix} v_1 & v_2 \\ v_3 & v_4 \end{bmatrix} = -\gamma_\omega \begin{bmatrix} \varphi_{M0}^2 & -\varphi_{M0}\varphi_{T0} \\ -\varphi_{M0}\varphi_{T0} & \varphi_{T0}^2 \end{bmatrix} - \gamma_{rs} \begin{bmatrix} w_{M0}^2 + w_{M0}i_{Ms0} & (i_{Ms0} - w_{M0})w_{T0} \\ w_{M0}(i_{Ts0} - w_{T0}) & w_{T0}^2 + w_{T0}i_{Ts0} \end{bmatrix}$$

and

$$\begin{cases} \varphi_{M0} = \frac{c\omega_{\psi 0}}{\omega_{\psi 0}^2 + c^2} |\psi_\mu^*| \\ \varphi_{T0} = -\frac{\omega_{\psi 0}}{\omega_{\psi 0}^2 + c^2} |\psi_\mu^*| \\ w_{M0} = \frac{c\omega_{\psi 0}i_{Ts0} - \omega_{\psi 0}^2 i_{Ms0}}{\omega_{\psi 0}^2 + c^2} \\ w_{T0} = -\frac{c\omega_{\psi 0}i_{Ms0} + \omega_{\psi 0}^2 i_{Ts0}}{\omega_{\psi 0}^2 + c^2} \\ \hat{e}_{M0} = \omega_{\psi 0} \hat{\psi}_{T\mu 0} = 0 \\ \hat{e}_{T0} = -\omega_{\psi 0} \hat{\psi}_{M\mu 0} = -\omega_{\psi 0} |\psi_\mu^*| \end{cases} \quad (\text{A.3})$$

When only the stability of the speed estimation is concerned, it is sufficient to consider the model (A.2) with $\delta \tilde{r}_s = 0$ and $\gamma_{rs} = 0$, and the stability of the speed estimation is revealed by the stability of the 5×5 sub-matrix of A_0

$$A_{0,5} = \begin{bmatrix} -k & \omega_{\psi 0} & 1 & 0 & 0 \\ -\omega_{\psi 0} & -k & 0 & 1 & 0 \\ v_1 - k_2 & v_2 & -\alpha & \omega_{sl0} & -\hat{e}_{T0} \\ v_3 & v_4 - k_2 & -\omega_{sl0} & -\alpha & \hat{e}_{M0} \\ -\gamma_\omega \varphi_{M0} & -\gamma_\omega \varphi_{T0} & 0 & 0 & 0 \end{bmatrix} \quad (\text{A.4})$$

APPENDIX B STABILITY PROOF OF (6)

According to [64, Lemma 3 and Corollary 1-2], the virtual system (6) is stable if there exists a positive definite matrix P such that i) $P [I \quad cI] = [I \quad 0]^T$, and ii) the matrix $Q = -(K_0^T P + PK_0)$ is positive definite, with

$$K_0 = \begin{bmatrix} -kI & I \\ -k_2 I & -\alpha I + \omega J \end{bmatrix}.$$

The first condition is satisfied if we choose P as

$$P = \begin{bmatrix} (1+c^2)I & -cI \\ -cI & I \end{bmatrix} \quad (\text{B.1})$$

The positive-definiteness of the resulting matrix

$$Q = \begin{bmatrix} [2ck_2 - 2k(c^2 + 1)]I & C_0 I - c\omega J \\ C_0 I + c\omega J & (-2\alpha - 2c)I \end{bmatrix} \quad (\text{B.2})$$

with $C_0 = \alpha c + c^2 + ck - k_2 + 1$, would be established by Sylvester's criterion, if we choose k, k_2, c to satisfy

$$\begin{cases} k = c + \alpha c^2 + c^3 + k' \\ k' > \frac{1}{4}\omega^2 \frac{c^2}{c+\alpha} \\ k_2 = 1 + \alpha c + c^2 + ck \end{cases} \quad (\text{B.3})$$

Remark: Considering (B.3), one possible choice of k, k_2, c is

$$\begin{cases} c = c'/|\omega|, c' > 0 \\ k' = \frac{1}{4}\omega^2 \frac{c^2}{c+\alpha} + 1 = \frac{1}{4}\frac{c'^2}{c+\alpha} + 1 \\ k = c + \alpha c^2 + c^3 + k' \\ k_2 = 1 + \alpha c + c^2 + ck \end{cases} \quad (\text{B.4})$$

which is found to have the potential to attain stable speed estimation over all working conditions, if c' is sufficiently large (see Fig. 11). However, the relative stability is very poor and is further deteriorated with a larger c' .

APPENDIX C STABILITY VERIFICATION OF RESISTANCES IDENTIFICATION IN MOTORING REGION

We cannot perform steady-state linearized model based stability analysis when a time-varying flux modulus command is imposed, for it results in a time-varying homogeneous matrix of the linearized model. In this appendix, the simulation studies are conducted to verify the effectiveness of the proposed sensorless control with stator and rotor resistances

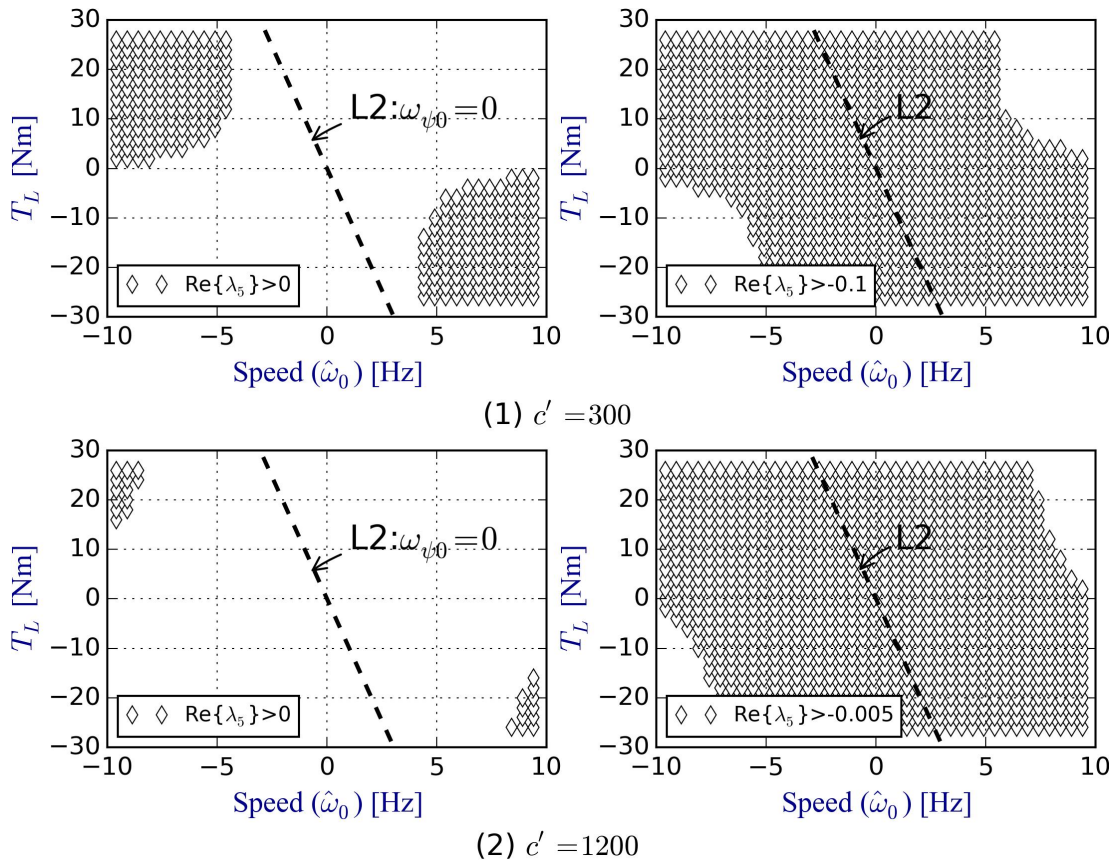


Fig. 11. Illustration of stability margin of $A_{0,5}$ with the positive-definiteness based coefficients choice (B.4).

identification. To this end, the torque-speed characteristics in motoring region (see Fig. 12b) are obtained by a sweeping of speed command and load torque. The waveforms of \hat{r}_s , \hat{r}_{req} , ω , $\hat{\omega}$, $|\psi_\mu^*|$, $|\psi_\mu|$ and the electromagnetic torque T_{em} are sketched in Fig 12a. The updating interval of working point is 5 sec.

In Fig. 12a, it is found that the value of the estimated stator resistance is biased from the actual one when the speed becomes high. This is because the accuracy of the approximation of the stator current becomes low at high frequency stator excitations. In fact, the mismatch of stator resistance estimation is remarkable when rotor speed becomes high enough, but it is not causing obvious detuned estimation of rotor speed or of rotor resistance. This is due to the low sensitivity of r_s in high speed region [62], [65]. As for the estimation of r_{req} , it is observed the convergence rate becomes lower when the load torque is high and the speed is low, but the estimation will converge given enough time. The resultant conclusion is that the proposed adaptive observer and sensorless control works stably for most of the motoring operations, and the inclusion of r_{req} estimation is not causing stability issues. In fact, it has been reported in several papers [33], [37], [43] that the rotor resistance error will not lead to instability.

REFERENCES

- [1] L. Harnefors, "Instability phenomena and remedies in sensorless indirect field oriented control," *Power Electronics, IEEE Transactions on*, vol. 15, no. 4, pp. 733–743, Jul 2000.
- [2] R. Marino, S. Peresada, and P. Tomei, "Exponentially convergent rotor resistance estimation for induction motors," *IEEE Transactions on Industrial Electronics*, vol. 42, no. 5, pp. 508–515, Oct 1995.
- [3] C. Attaianese, G. Tomasso, A. Damiano, A. D. Marongiu, and A. Perfetto, "On line estimation of speed and parameters in induction motor drives," in *Industrial Electronics, 1997. ISIE '97., Proceedings of the IEEE International Symposium on*, Jul 1997, pp. 1054–1059 vol.3.
- [4] V. Vasić, S. N. Vukosavic, and E. Levi, "A stator resistance estimation scheme for speed sensorless rotor flux oriented induction motor drives," *Energy Conversion, IEEE Transactions on*, vol. 18, no. 4, pp. 476–483, 2003.
- [5] H. Kubota, K. Matsuse, and T. Nakano, "Dsp-based speed adaptive flux observer of induction motor," *IEEE Transactions on Industry Applications*, vol. 29, no. 2, pp. 344–348, Mar 1993.
- [6] L. Zhao, J. Huang, J. Chen, and M. Ye, "A parallel speed and rotor time constant identification scheme for indirect field oriented induction motor drives," *IEEE Transactions on Power Electronics*, vol. 31, no. 9, pp. 6494–6503, Sept 2016.
- [7] P. L. Jansen and R. D. Lorenz, "Transducerless field orientation concepts employing saturation-induced saliences in induction machines," *IEEE Transactions on Industry Applications*, vol. 32, no. 6, pp. 1380–1393, Nov 1996.
- [8] J.-I. Ha and S.-K. Sul, "Sensorless field-orientation control of an induction machine by high-frequency signal injection," *IEEE Transactions on Industry Applications*, vol. 35, no. 1, pp. 45–51, Jan 1999.
- [9] R. Marino, P. Tomei, and C. Verrelli, "Adaptive control for speed-sensorless induction motors with uncertain load torque and rotor resistance," *International Journal of Adaptive Control and Signal Processing*, vol. 19, no. 9, pp. 661–685, 2005.
- [10] R. Marino, P. Tomei, and C. M. Verrelli, "An adaptive tracking control from current measurements for induction motors with uncertain load torque and rotor resistance," *Automatica*, vol. 44, no. 10, pp. 2593–2599, 2008.
- [11] K. Akatsu and A. Kawamura, "Online rotor resistance estimation using the transient state under the speed sensorless control of induction motor," *IEEE Transactions on Power Electronics*, vol. 15, no. 3, pp. 553–560, May 2000.

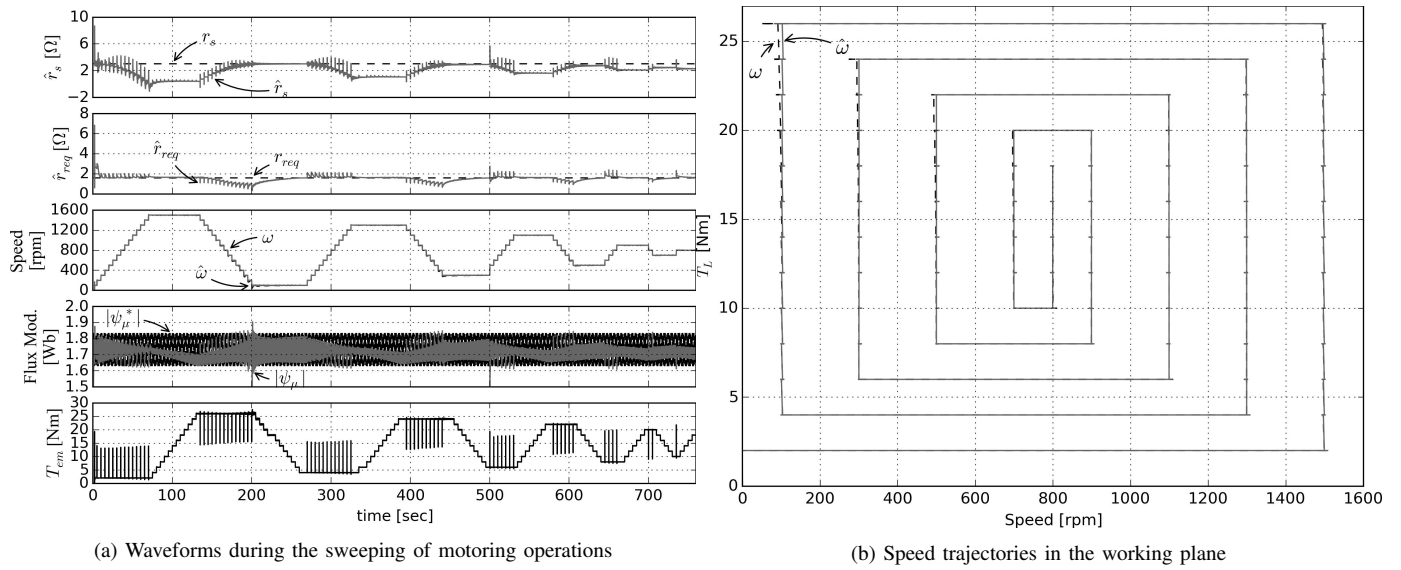


Fig. 12. Simulated verification of the stability of the proposed simultaneous resistances identification in speed sensorless drives over the motoring working plane.

- [12] —, "Sensorless very low-speed and zero-speed estimations with online rotor resistance estimation of induction motor without signal injection," *Industry Applications, IEEE Transactions on*, vol. 36, no. 3, pp. 764–771, 2000.
- [13] L. Zhen and L. Xu, "Sensorless field orientation control of induction machines based on a mutual mras scheme," *IEEE Transactions on Industrial Electronics*, vol. 45, no. 5, pp. 824–831, 1998.
- [14] K. Kubota and K. Matsuse, "Speed sensorless field-oriented control of induction motor with rotor resistance adaptation," *Industry Applications, IEEE Transactions on*, vol. 30, no. 5, pp. 1219–1224, Sep 1994.
- [15] H. Tajima, G. Guidi, and H. Umida, "Consideration about problems and solutions of speed estimation method and parameter tuning for speed-sensorless vector control of induction motor drives," *Industry Applications, IEEE Transactions on*, vol. 38, no. 5, pp. 1282–1289, 2002.
- [16] H. Rasmussen, P. Vadstrup, and H. Borsting, "Full adaptive backstepping design of a speed sensorless field oriented controller for an induction motor," in *Industry Applications Conference, 2001. Thirty-Sixth IAS Annual Meeting. Conference Record of the 2001 IEEE*, vol. 4, Sept 2001, pp. 2601–2606 vol.4.
- [17] I.-J. Ha and S.-H. Lee, "An online identification method for both stator- and rotor resistances of induction motors without rotational transducers," *IEEE Transactions on Industrial Electronics*, vol. 47, no. 4, pp. 842–853, Aug 2000.
- [18] K. Wang, B. Chen, G. Shen, W. Yao, K. Lee, and Z. Lu, "Online updating of rotor time constant based on combined voltage and current mode flux observer for speed-sensorless ac drives," *IEEE Transactions on Industrial Electronics*, vol. 61, no. 9, pp. 4583–4593, Sept 2014.
- [19] G. Yang and T. H. Chin, "Adaptive-speed identification scheme for a vector-controlled speed sensorless inverter-induction motor drive," *IEEE Transactions on Industry Applications*, vol. 29, no. 4, pp. 820–825, Jul 1993.
- [20] P. Vaclavek and P. Blaha, "Lyapunov-function-based flux and speed observer for ac induction motor sensorless control and parameters estimation," *IEEE Transactions on Industrial Electronics*, vol. 53, no. 1, pp. 138–145, Feb 2005.
- [21] B. Karanayil, M. F. Rahman, and C. Grantham, "Online stator and rotor resistance estimation scheme using artificial neural networks for vector controlled speed sensorless induction motor drive," *IEEE Transactions on Industrial Electronics*, vol. 54, no. 1, pp. 167–176, Feb 2007.
- [22] S. E. Rezgui, S. Legrioui, A. Mehdi, and H. Benalla, "Robust im control with mras-based speed and parameters estimation with ann using exponential reaching law," in *Control, Decision and Information Technologies (CoDIT), 2014 International Conference on*, Nov 2014, pp. 477–482.
- [23] M. Barut, S. Bogosyan, and M. Gokasan, "Switching ekf technique for rotor and stator resistance estimation in speed sensorless control of ims," *Energy Conversion and Management*, vol. 48, no. 12, pp. 3120 – 3134, 2007. [Online]. Available: <http://www.sciencedirect.com/science/article/pii/S0196890407001252>
- [24] —, "Experimental evaluation of braided ekf for sensorless control of induction motors," *IEEE Transactions on Industrial Electronics*, vol. 55, no. 2, pp. 620–632, Feb 2008.
- [25] M. Barut, "Bi input-extended kalman filter based estimation technique for speed-sensorless control of induction motors," *Energy Conversion and Management*, vol. 51, no. 10, pp. 2032 – 2040, 2010. [Online]. Available: <http://www.sciencedirect.com/science/article/pii/S0196890410001032>
- [26] M. Barut, R. Demir, E. Zerdali, and R. Inan, "Real-time implementation of bi input-extended kalman filter-based estimator for speed-sensorless control of induction motors," *IEEE Transactions on Industrial Electronics*, vol. 59, no. 11, pp. 4197–4206, Nov 2012.
- [27] G. Besançon, J. de Leon-Morales, and O. Huerta-Guevara, "On adaptive observers for state affine systems and application to synchronous machines," in *Decision and Control, 2003. Proceedings. 42nd IEEE Conference on*, vol. 3, Dec 2003, pp. 2192–2197 Vol.3.
- [28] G. Besançon, J. D. Len-Morales, and O. Huerta-Guevara, "On adaptive observers for state affine systems," *International Journal of Control*, vol. 79, no. 6, pp. 581–591, 2006. [Online]. Available: <http://dx.doi.org/10.1080/00207170600552766>
- [29] P. C. Young, *Recursive estimation and time-series analysis: An introduction for the student and practitioner*, 2nd ed. Springer Science & Business Media (Harvard), 2011.
- [30] L. Ljung, "Asymptotic behavior of the extended kalman filter as a parameter estimator for linear systems," *IEEE Transactions on Automatic Control*, vol. 24, no. 1, pp. 36–50, Feb 1979.
- [31] L. Harnefors and M. Hinkkanen, "Stabilization methods for sensorless induction motor drives — a survey," *IEEE Journal of Emerging and Selected Topics in Power Electronics*, vol. 2, no. 2, pp. 132–142, June 2014.
- [32] S. Sangwongwanich, S. Suwankawin, S. Po-ngam, and S. Koonlaboon, "A unified speed estimation design framework for sensorless ac motor drives based on positive-real property," in *2007 Power Conversion Conference - Nagoya*, April 2007, pp. 1111–1118.
- [33] S. Suwankawin and S. Sangwongwanich, "A speed-sensorless im drive with decoupling control and stability analysis of speed estimation," *IEEE Transactions on Industrial Electronics*, vol. 49, no. 2, pp. 444–455, Apr 2002.
- [34] Z. Qu, M. Hinkkanen, and L. Harnefors, "Gain scheduling of a full-order observer for sensorless induction motor drives," *IEEE Transactions on Industry Applications*, vol. 50, no. 6, pp. 3834–3845, Nov 2014.
- [35] L. Harnefors and M. Hinkkanen, "Complete stability of reduced-order and full-order observers for sensorless im drives," *IEEE Transactions on Industrial Electronics*, vol. 55, no. 3, pp. 1319–1329, March 2008.
- [36] H. Kubota, I. Sato, Y. Tamura, K. Matsuse, H. Ohta, and Y. Hori, "Regenerating-mode low-speed operation of sensorless induction motor

- drive with adaptive observer," *IEEE Transactions on Industry Applications*, vol. 38, no. 4, pp. 1081–1086, Jul 2002.
- [37] M. Tsuji, S. Chen, K. Izumi, and E. Yamada, "A sensorless vector control system for induction motors using q-axis flux with stator resistance identification," *IEEE Transactions on Industrial Electronics*, vol. 48, no. 1, pp. 185–194, Feb 2001.
- [38] M. Hinkkanen, "Analysis and design of full-order flux observers for sensorless induction motors," *IEEE Transactions on Industrial Electronics*, vol. 51, no. 5, pp. 1033–1040, Oct 2004.
- [39] E. Etien, C. Chaigne, and N. Bensiali, "On the stability of full adaptive observer for induction motor in regenerating mode," *IEEE Transactions on Industrial Electronics*, vol. 57, no. 5, pp. 1599–1608, May 2010.
- [40] M. Hinkkanen and J. Luomi, "Stabilization of regenerating-mode operation in sensorless induction motor drives by full-order flux observer design," *IEEE Transactions on Industrial Electronics*, vol. 51, no. 6, pp. 1318–1328, Dec 2004.
- [41] M. S. Zaky, "Stability analysis of speed and stator resistance estimators for sensorless induction motor drives," *IEEE Transactions on Industrial Electronics*, vol. 59, no. 2, pp. 858–870, Feb 2012.
- [42] M. Zaky and M. Metwaly, "Sensorless torque/speed control of induction motor drives at zero and low frequency with stator and rotor resistance estimation," *IEEE Journal of Emerging and Selected Topics in Power Electronics*, vol. PP, no. 99, pp. 1–1, 2016.
- [43] M. Saejia and S. Sangwongwanich, "Averaging analysis approach for stability analysis of speed-sensorless induction motor drives with stator resistance estimation," *IEEE Transactions on Industrial Electronics*, vol. 53, no. 1, pp. 162–177, Feb 2006.
- [44] C.-M. Chang and C.-H. Liu, "A new mras based strategy for simultaneous estimation and control of a sensorless induction motor drive," *Journal of the Chinese Institute of Engineers*, vol. 33, no. 3, pp. 451–462, 2010.
- [45] J. Chen and J. Huang, "Online decoupled stator and rotor resistances adaptation for speed sensorless induction motor drives by a time-division approach," *IEEE Transactions on Power Electronics*, vol. 32, no. 6, pp. 4587–4599, June 2017.
- [46] L. Harnefors, "Globally stable speed-adaptive observers for sensorless induction motor drives," *IEEE Transactions on Industrial Electronics*, vol. 54, no. 2, pp. 1243–1245, April 2007.
- [47] R. Marino, S. Peresada, and P. Tomei, "On-line stator and rotor resistance estimation for induction motors," *Control Systems Technology, IEEE Transactions on*, vol. 8, no. 3, pp. 570–579, 2000.
- [48] S. H. Jeon, K. K. Oh, and J. Y. Choi, "Flux observer with online tuning of stator and rotor resistances for induction motors," *Industrial Electronics, IEEE Transactions on*, vol. 49, no. 3, pp. 653–664, 2002.
- [49] T. Abbasian, F. Salmasi, and M. Yazdanpanah, "Stability analysis of sensorless im based on adaptive feedback linearization control with unknown stator and rotor resistances," in *Industry Applications Conference, 2005. Forty-fourth IAS Annual Meeting. Conference Record of the 2005*, vol. 2. IEEE, 2005, pp. 985–992.
- [50] G. A. Markadeh, M. Hajian, J. Soltani, and S. Hosseini, "Maximum torque per ampere control of sensorless induction motor drives with dc offset and parameter compensation," *Energy Conversion and Management*, vol. 51, no. 7, pp. 1354 – 1362, 2010. [Online]. Available: <http://www.sciencedirect.com/science/article/pii/S0196890409004865>
- [51] R. Marino, P. Tomei, and C. M. Verrelli, "Tracking control for sensorless induction motors with uncertain load torque and resistances," in *Nonlinear Control Systems*, 2010, pp. 771–776.
- [52] R. Marino, T. Patrizio, and M. C. Verrelli, *AC Electric Motors Control: Advanced Design Techniques and Applications*. Wiley Online Library, 2013, ch. Adaptive Output Feedback Control of Induction Motors, pp. 158–187.
- [53] R. Marino, P. Tomei, and C. M. Verrelli, "A new flux observer for induction motors with on-line identification of load torque and resistances," in *18th IFAC World Congress, Milano, Italy*, vol. 18, 2011, pp. 6172–6177.
- [54] C. Verrelli, A. Savoia, M. Mengoni, R. Marino, P. Tomei, and L. Zarri, "On-line identification of winding resistances and load torque in induction machines," *Control Systems Technology, IEEE Transactions on*, vol. 22, no. 4, pp. 1629–1637, July 2014.
- [55] R. Marino and P. Tomei, "Global adaptive observers for nonlinear systems via filtered transformations," *IEEE Transactions on Automatic Control*, vol. 37, no. 8, pp. 1239–1245, Aug 1992.
- [56] G. R. Slemon, "Modelling of induction machines for electric drives," *IEEE Transactions on Industry Applications*, vol. 25, no. 6, pp. 1126–1131, Nov 1989.
- [57] H. Hofmann and S. R. Sanders, "Speed-sensorless vector torque control of induction machines using a two-time-scale approach," *IEEE Transactions on Industry Applications*, vol. 34, no. 1, pp. 169–177, Jan 1998.
- [58] P. Kudva and K. S. Narendra, "Synthesis of an adaptive observer using lyapunov's direct method," *International Journal of Control*, vol. 18, no. 6, pp. 1201–1210, 1973. [Online]. Available: <http://dx.doi.org/10.1080/00207177308932593>
- [59] J. Chiasson, "Nonlinear controllers for an induction motor," *Control Engineering Practice*, vol. 4, no. 7, pp. 977 – 990, 1996. [Online]. Available: <http://www.sciencedirect.com/science/article/pii/0967066196000974>
- [60] P. Vas, *Sensorless vector and direct torque control*. Oxford University Press, USA, 1998.
- [61] D. Telford, M. W. Dunnigan, and B. W. Williams, "Online identification of induction machine electrical parameters for vector control loop tuning," *IEEE Transactions on Industrial Electronics*, vol. 50, no. 2, pp. 253–261, Apr 2003.
- [62] F. Jadot, F. Malrait, J. Moreno-Valenzuela, and R. Sepulchre, "Adaptive regulation of vector-controlled induction motors," *Control Systems Technology, IEEE Transactions on*, vol. 17, no. 3, pp. 646–657, 2009.
- [63] F. Filippietti, G. Franceschini, C. Tassoni, and P. Vas, "Ai techniques in induction machines diagnosis including the speed ripple effect," *IEEE Transactions on Industry Applications*, vol. 34, no. 1, pp. 98–108, Jan 1998.
- [64] K. S. Narendra and P. Kudva, "Stable adaptive schemes for system identification and control - part ii," *IEEE Transactions on Systems, Man, and Cybernetics*, vol. SMC-4, no. 6, pp. 552–560, Nov 1974.
- [65] J. Chen, J. Huang, and M. Ye, "Totally adaptive observer for speed sensorless induction motor drives: Simply a cost of extra energy consumption," in *2017 IEEE International Electric Machines and Drives Conference (IEMDC)*, May 2017, pp. 1–7.



Jiahao Chen was born in Wenzhou, China, in 1991. He received the B.Sc. degree from Zhejiang University, Hangzhou, China, in 2014, and is now a Ph.D. candidate at the Institute of Electrical Engineering in Zhejiang University, both in electrical engineering. His research interests include parameter estimation and motion control of electric motors.



Jin Huang received the B.Sc. degree in electrical engineering from Zhejiang University, Hangzhou, China, in 1982, and the Ph.D. degree in electrical engineering from the National Polytechnic Institute of Toulouse, Toulouse, France, in 1987. From 1987 to 1994, he was an Associate Professor with the College of Electrical Engineering, Zhejiang University. Since 1994, he has been a Professor at Zhejiang University. His research interests include electrical machine, ac drives, multiphase machine, and motor parameter identification.